Electronic Supplementary Material (ESI) for Nanoscale.

Supporting Information

An Electrochemical Biosensor Exploiting Binding-Induced Changes In Electron Transfer of Electrode-Attached DNA Origami to Detect Hundred Nanometer-Scale Targets

Netzahualcóyotl Arroyo-Currás,[b] *Muaz Sadeia,[a] Alexander K. Ng,[a] Yekaterina Fyodorova,[a] Natalie Williams,[a] Tammy Afif,[a]* Chao-Min Huang,[d] Nathan Ogden,[c] Roberto C. Andresen Eguiluz,[c] Hai-Jun Su,[d] Carlos E. Castro,[d] Kevin W. Plaxco[c] and Philip S. Lukeman*[a]

[a] Department of Chemistry, St. John's University, Queens, NY 11439, United States

[b] Department of Pharmacology and Molecular Sciences, Johns Hopkins University School of Medicine, Baltimore, MD 21205, United States

[c] Department of Chemistry and Biochemistry, Center for Bioengineering and Department of Chemical Engineering, University of California Santa Barbara, Santa Barbara, CA 93106, United States

[d]Department of Mechanical and Aerospace Engineering/Biophysics Graduate Program, The Ohio State University, Columbus, Ohio 43210, United States

Italicized co-authors are undergraduates.

***Corresponding Author**

Philip S. Lukeman, Associate Professor

Department of Chemistry, St. Albert Hall
St. John's University
8000 Utopia Parkway, Queens, NY 11439, USA.
lukemanp@stjohns.edu
+1 718 990 8322

Table of Contents

Fig. SA. The ability of the electrode-bound receptor to specifically bind to its designed targets can be replicated when free in bulk solution.

We illustrate this via gel-shift analyses of the receptor and its targets. By first measuring the intrinsic fluorescence of the redox reporter, methylene blue, we evaluated the result of challenging the receptor with the anti strand, which displaces the reporter from the receptor, eliminating its corresponding band in the gel (**A**, lane 3 versus 10). This displacement produces a lower molecular weight band corresponding to free reporter-containing strands (blue-dashed circles). To demonstrate the specific binding of targets we stained the same gel with SYBR gold, which binds to all DNA-containing analytes (**B**). Doing so we noted that the band corresponding to R shifted upon challenging with the targets K1 or K3 but remains at the same mobility when challenged with the non-binding control K_{NC}.
The Lanes are 1) 1 kb DNA ladder; 2) the m13mp18 plasmid; 3) R; 4) K_{NC}; 5) K_{NC}+R 6) K1; 7) K1+R; 8) K3; 9) K3+R; 10) R+anti strand; 11) anti strand; 12) MB strand

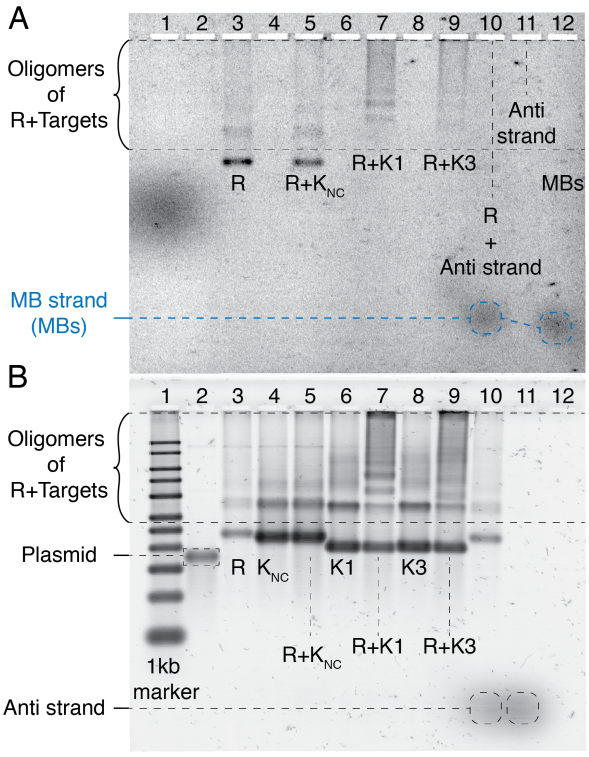

More detail: We validated the binding of receptor (R) when free in solution by challenging it with targets K_{NC}, K1 and K3 and characterizing the resulting complexes using gel electrophoresis. **A**) Imaging via the fluorescence emission of methylene blue (MB) (excitation at 635 nm and detection > 665 nm) we confirmed that, as expected, the K_{NC} target, which is not complementary to our receptor, does not bind; this is evidenced by the absence of a band shift (lanes 3 versus 5). In contrast, the band indicative of free receptor disappears when the target K1 or K3 are present (lanes 3 versus 7,9); instead we observe the formation of oligomers under these conditions. Displacement of the reporter modified strands by challenging the MB-containing duplexes in the receptor with an anti-strand, which causes the disappearance of the receptor band and the appearance of free MB strands when visualized by MB fluorescence (lanes 3 versus 10). No detectable MB strand release occurs, in contrast, upon challenge with any of the receptor's three targets. The large stain in lane 1 is from the 1 kbp markersolution's loading dye. **B**) Here we show the same gel but after staining with SYBR gold (exciting at λ = 473 nm, detecting at 560-580 nm) to reveal all DNA-containing species, which confirms the presence of a single prominent band corresponding to the receptor (lane 3), target K_{NC} (lane 4), target K1 (lane 6) or target K3 (lane 8). The band corresponding to the receptor disappears when challenged with either target K1 or target K3. The gels were made of 1% agarose in HEPES buffer containing 6 mM magnesium ions and ran at 25º C. The concentrations for the binding assays were 1 nM (R) and 2 nM (K_{NC}, K1 and K3). For reference, the original, unannotated gel images are included in **Fig. S9**.

Fig. SB. AFM shows that origami receptors and targets are the expected size and shape.

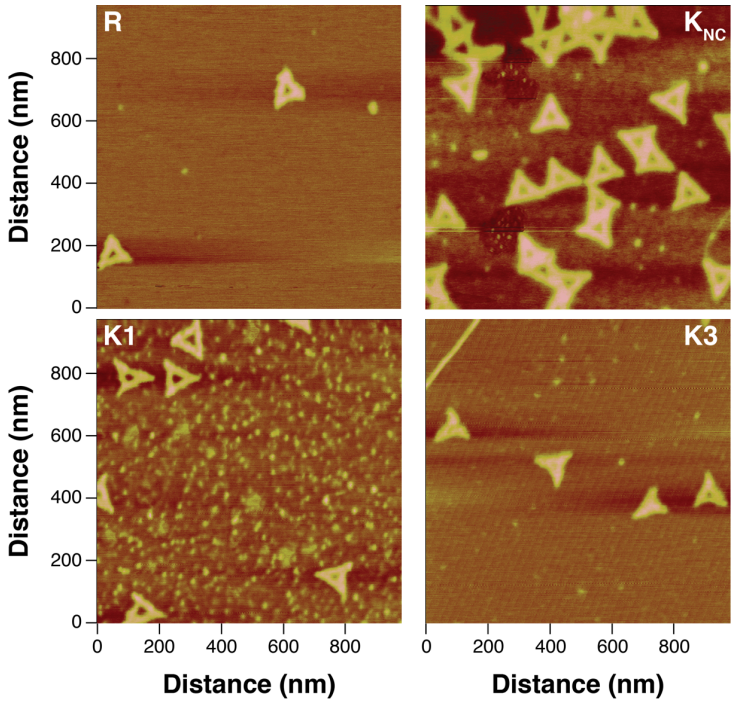

We performed AFM analyses using tapping-mode in air of R, K_{NC}, K1 and K3. We observed that the origami were, as predicted, 2nm high, 120 nm sided triangles.

Despite significant effort, we have not been able to isolate and AFM image K3:R or K1:R dimer complexes, which form multimers when in free solution. However, we are confident that the R and K1 or K3 can bind in a 1:1 face sharing manner when R is site-isolated on the electrode surface. See the supporting info in this paper[1] where similar origami triangles can be observed stacking on top of each other in the same geometry *when site-isolated on a surface*.

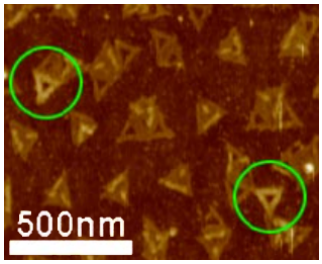

AFM image of triangle origami with the same overall scaffold path, similar dimensions and face-sharing binding site design as our receptor and targets. Green circles show that face-sharing ('double height') origami dimers can form when site-isolated on the surface.

Future versions of this Receptor:Target system with steric hindrance aimed at blocking solution multimerization would likely allow us to isolate dimers.

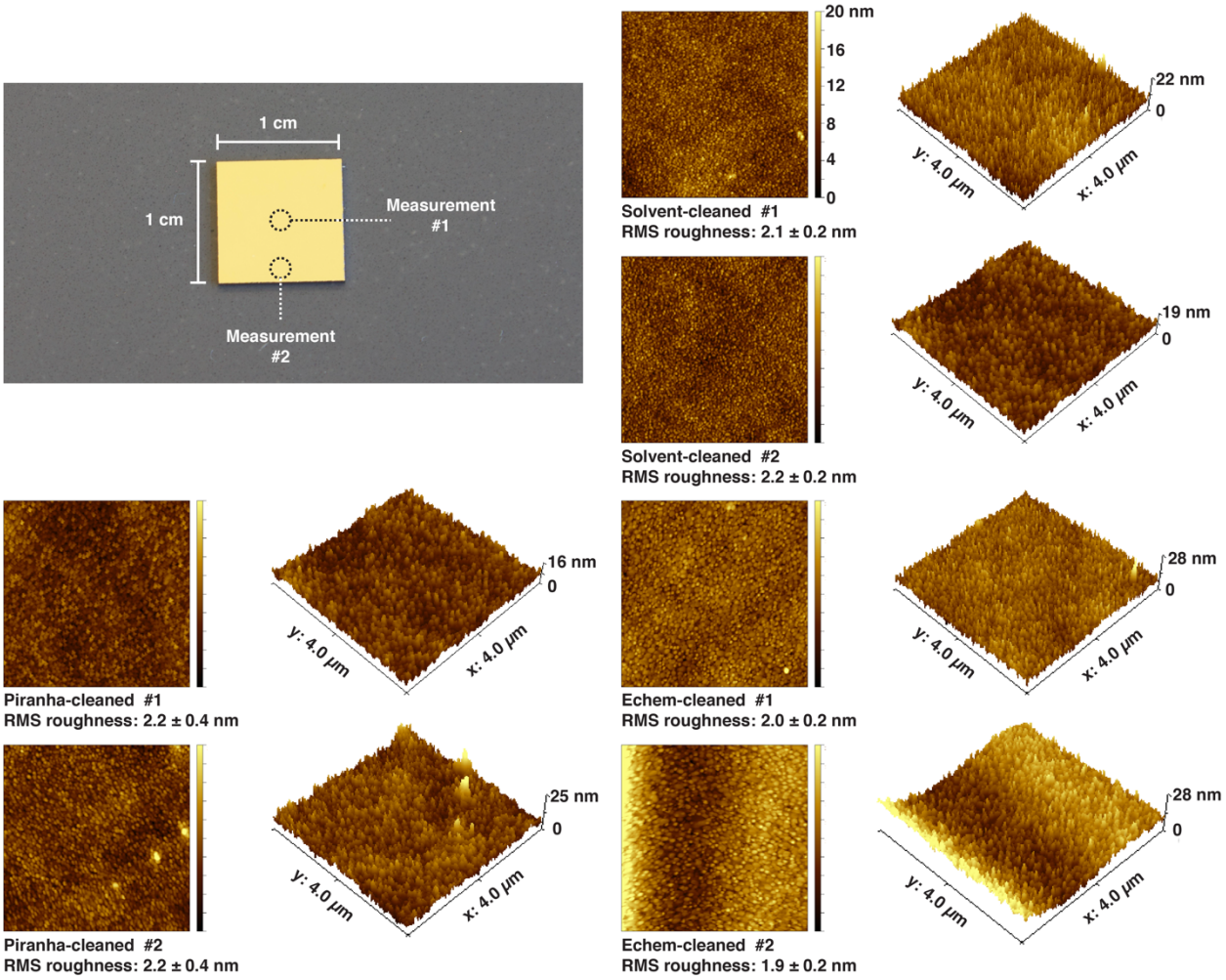

Fig. S1. AFM characterization of substrates prepared by e-beam deposition

With the goal of functionalizing flat, smooth gold surfaces with DNA origami, we studied the surface roughness produced by different cleaning protocols on gold substrates prepared by e-beam deposition. We evaluated 3 different cleaning protocols: 1) only solvent-treated surfaces (acetone, 2-propanol, then dried in air); 2) solvent-treated, Piranha-treated (hydrogen peroxide to sulfuric acid ratio of 3:1, 1 min immersion); 3) solvent-treated, electrochemically-treated via cyclic voltammetry in 0.5 M sulfuric acid. Our measurements indicated that the surface roughness was not significantly affected by these treatments when comparing the same batch of substrates (coming from the same wafer). To acquire these images we used an Asylum AFM model MFP-3D-Bio in contact mode. The images are 4.0 by 4.0 µm and 512 by 512 pixels, obtained at a scanning rate of 0.7 Hz.

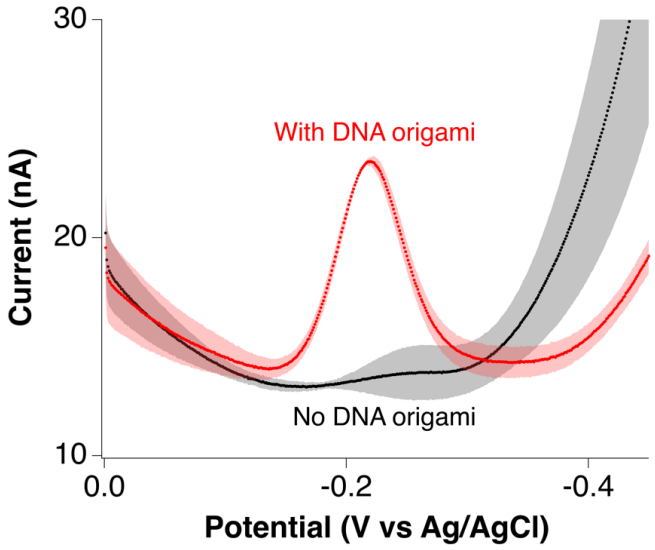

Fig. S2. Square-wave voltammograms of 1,6-hexanedithiol-monolayer-coated substrates with and without DNA origami

Our functionalization protocol produces surfaces with good batch reproducibility. To illustrate this, here we show the average of 3 substrates modified with (black) the 1,6-hexanedithiol monolayer and 3 substrates with (red) both such a monolayer and DNA origami. The shaded areas represent the standard deviation between electrodes.

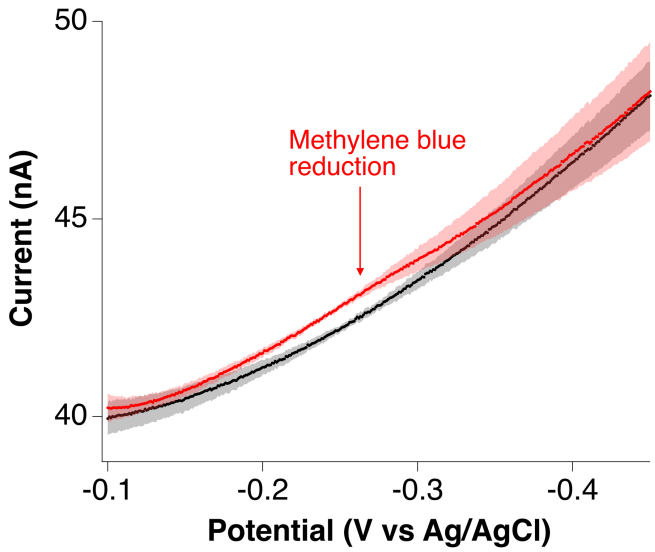

Fig. S3. Square-wave voltammograms of 1-mercapto-6-hexanol-coated substrates with and without DNA origami

The majority of electrochemical, DNA-based sensors use self-assembled monolayers of 1-mercapto-6-hexanol to passivate the surface of gold electrodes and, with this, prevent the occurrence of secondary redox reactions unrelated to the DNA. In this work, however, we observed that incubation of our sensors in solutions of 1-mercapto-6-hexanol produced porous monolayers that did not fully passivate the electrode surface. To illustrate this, here we show square-wave voltammograms of the monolayer recorded in the absence (black) and presence (red) of DNA origami. In both cases, we observe a sloping baseline that corresponds to the current generated by reducing solvated molecular oxygen on gold (which is present in the cell since our experiments were performed under a normal atmosphere of air). In addition to this effect, we also observed deposition of smaller quantities of DNA as determined by the area under the reduction peak (red arrow) obtained after incubation of the sensors in origami solutions for several hours (we tested 2-, 4-, 6- and 12-hour-long incubations). The voltammograms shown in Fig. S2, in contrast, were recorded on electrodes modified with 1,6-hexanedithiol SAMs and produced well defined reduction peaks. The shaded areas represent the standard deviation calculated from three measurements performed in three independent electrodes.

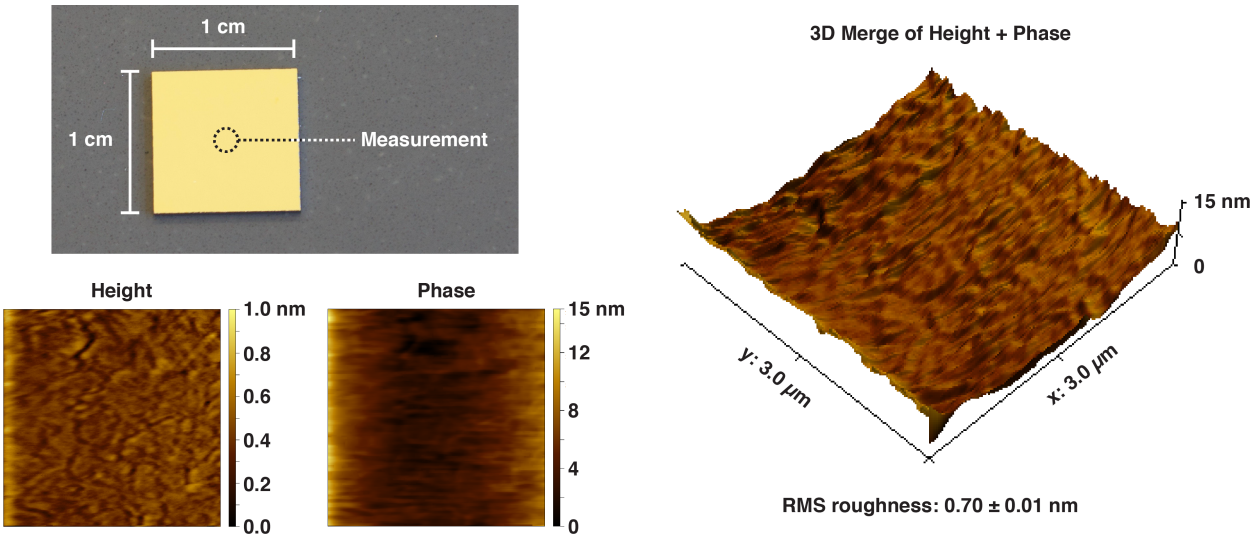

Fig. S4. AFM image of a typical 1,6-hexanedithiol-coated substrate

The RMS surface roughness of our substrates decreased ~ 33% after functionalization with 1,6-hexanedithiol, relative to the cleaned bare gold substrates presented in Fig. S1. Here, for example, we show AFM images of a monolayer-coated substrate immersed in a drop of 1X PBS (150 µL) recorded in contact mode. The images are 3.0 by 3.0 µm and 256 by 256 pixels and were obtained at a scanning rate of 0.7 Hz.

We note that previous reports have described the formation of multi-layers of dithiol SAMs, up to eight layers, on gold substrates[2-4]. However, these reports all used organic solvents (ethanol or n-hexanes) for dissolution of the dithiol reagents and for incubation of the gold substrates which may promote the formation of these multimeric species. Our work, in contrast, only employed aqueous solutions of 1,6-hexanedithiol and we observed no evidence of the existence of these multimers under our experimental conditions.

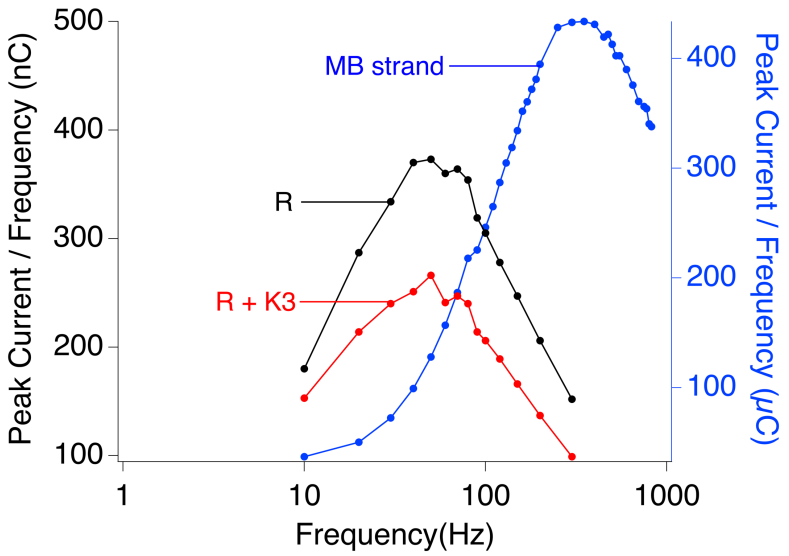

Fig. S5. Square-wave frequency analysis of origami-functionalized electrodes compared to free MB strand

We observed the largest peak current from square-wave voltammograms recorded at a square-wave frequency of 60 Hz, which coincidentally gives the largest relative signal change when our origami receptor (black) is bound to the triple-sided target (K3 in main text, red).

For reference, we show the same frequency analysis for methylene-blue-modified strands (blue), which undergo much faster electron transfer (i.e., the maximum is significantly shifted to faster frequencies relative to the x-axis).

The lack of a shoulder on the right side of the red trace confirms that target-binding on the electrode surface does not cause the release of methylene-blue-containing strands. This conclusion is supported by the gel electrophoresis data in Fig SA, showing that in bulk solution there is also no MB strand displacement by target binding to R.

We hypothesize that the binding event occurs in a manner similar to the schematic below

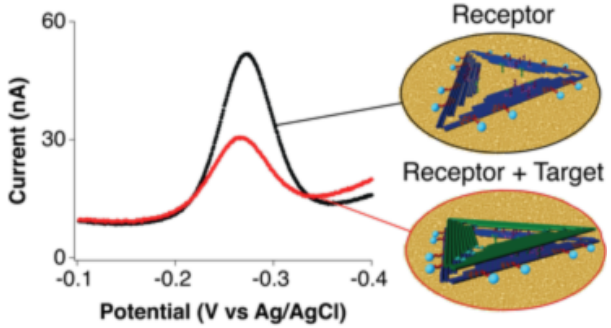

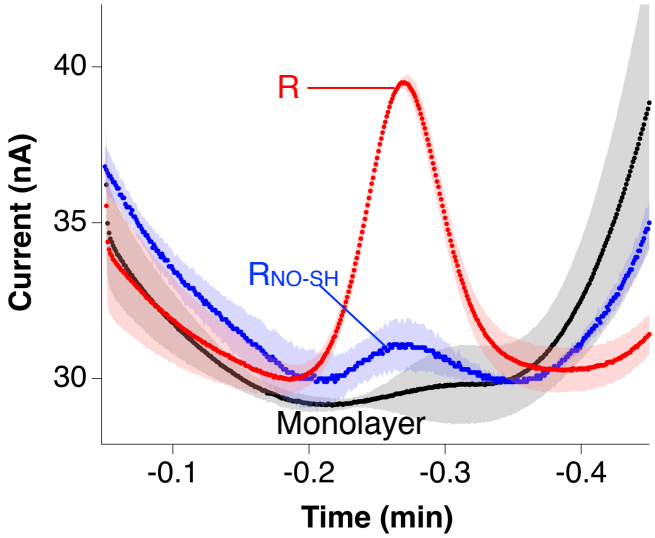

Fig. S6. Anchor thiols are necessary for effective and reliable surface attachment of DNA origami

Thiol-containing receptor DNA origami (Red curve - R) was covalently bound via disulfide bonds to the free thiol groups from the 1,6 hexanedithiol monolayer, producing 4 to 5-fold larger peak currents (red) and 3-fold lower sensor-to-sensor variability (shaded areas) relative to origami not specifically bound to the monolayer (Blue curve - $R_{NO\text{-}SH}$). These $R_{NO\text{-}SH}$ origami were identical to the receptor origami, displaying the same number and orientation of methylene blue strands and recognition sites, the sole difference being that the strands with thiols on the base of the receptor were replaced with 5'OH terminated strands. Data shown is the average of 3 replicates in parallel between R and $R_{NO\text{-}SH}$.

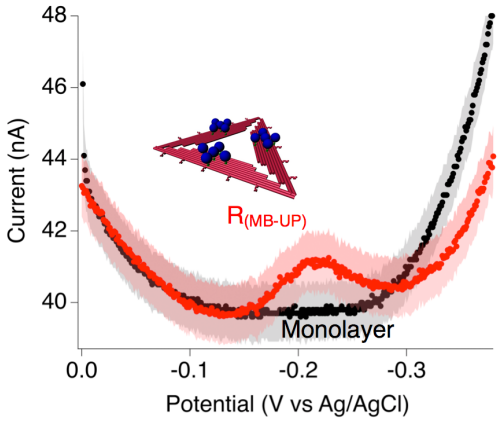

Fig. S7. The location and orientation of reporter-modified strands on surface-bound origami directly affect the currents measured via square-wave voltammetry

To demonstrate this, we made a variant of the receptor**, R(MB-UP)** with **fifteen** signal generating, redox-reporter-modified 24-mer DNA duplexes projecting **vertically** from the top of each-of-three edges in the same positions as the binding sites in the receptor. The sequences of these MB-displaying duplexes were the same as the side-pointing reporter duplexes in the receptor, and the thiol attachment pattern was the same as in the Receptor. While a 24mer duplex is ~8 nm long, taking into account the flexibility of linkers and nicks, we estimate that these triangles, if oriented as expected on the monolayer in the same manner as the receptor – that is, thiol-down, should display Methylene Blues a **minimum** of 3.5 nm further from the surface than the Receptor R. *This configuration produced 5-6-fold lower peak currents (red) relative to the receptor used in our work (**Fig. S6**), where the reporter-modified strands projected laterally from the outer edges of the origami triangles.* We explain this difference by invoking a tunneling argument: in the case where the reporter-modified strands project vertically from the top, the reporters are, in average, further away from the electrode surface than in the case where the reporter-modified strands project laterally from the edges, and thus undergo slower electron transfer per the formula[5]:

$$k^0(x) = k^0(x = 0) \int_x^\infty \mathrm{e}^{-\beta x}\, \mathrm{d}x$$

where k^0(x) is the rate of electron transfer for a surface-confined redox couple located at a distance x (in Å) from the electrode surface, k^0 (x = 0) is the rate of electron transfer for a surface-confined redox couple located at x = 0, and β is the exponential decay coefficient, which depends on the activation energy of the reaction and nature of the medium through which the electron transfers. The latter is on the order of 1.0 $Å^{-1}$ for systems involving tunneling across self-assembled alkane monolayers similar to that used here.

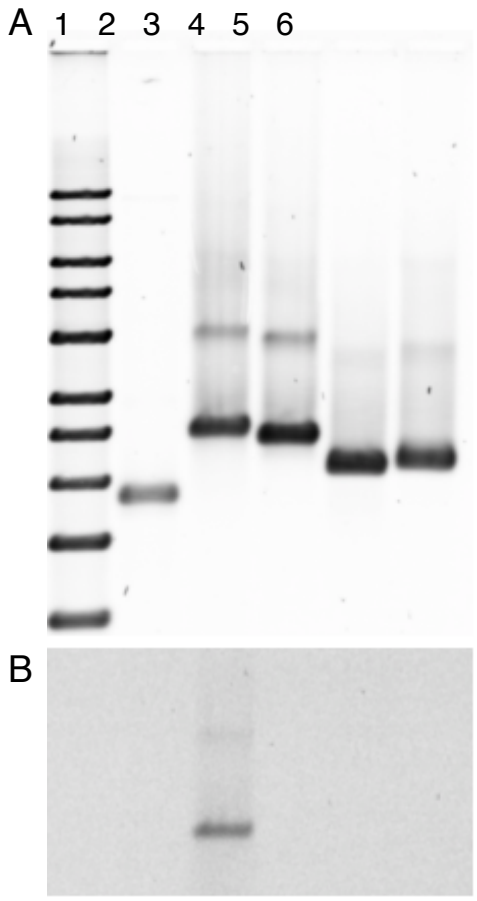

Fig S8. DNA origami assembly is confirmed via gel electrophoresis

The lanes are, from left-to-right:

1) 1 kb DNA ladder; 2) the m13mp18 plasmid; 3) R; 4) K_{NC}; 5) K1; and 6) K3.

A) SYBR gold-stained Agarose gel showing the bands produced by the triangle origami utilized in this work. We note the presence of small (< 5%) amounts of dimers, which are common in origami synthesis. **B**) The same gel as in A but pre-staining, imaged using the fluorescence emission of methylene blue. In agreement with our design, only the methylene blue-containing molecule, R (lane 3), is visible as a band.

Unstained, imaged using methylene blue fluorescence

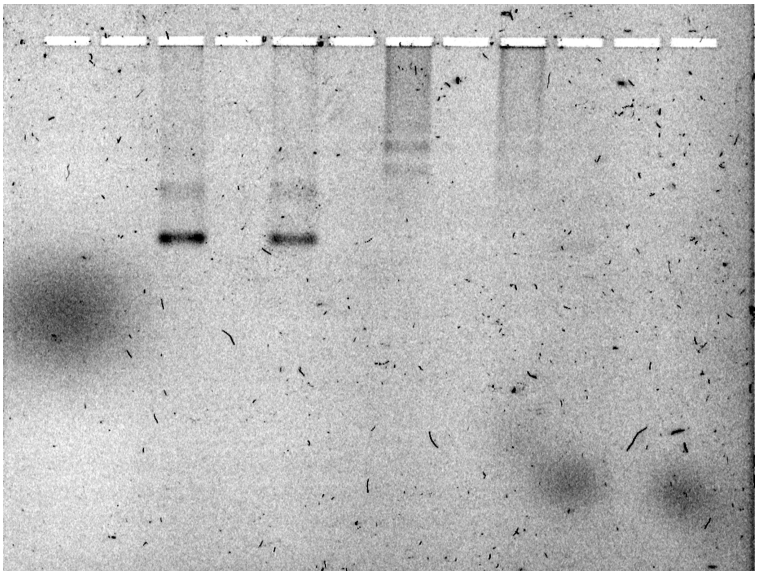

SYBR gold stained

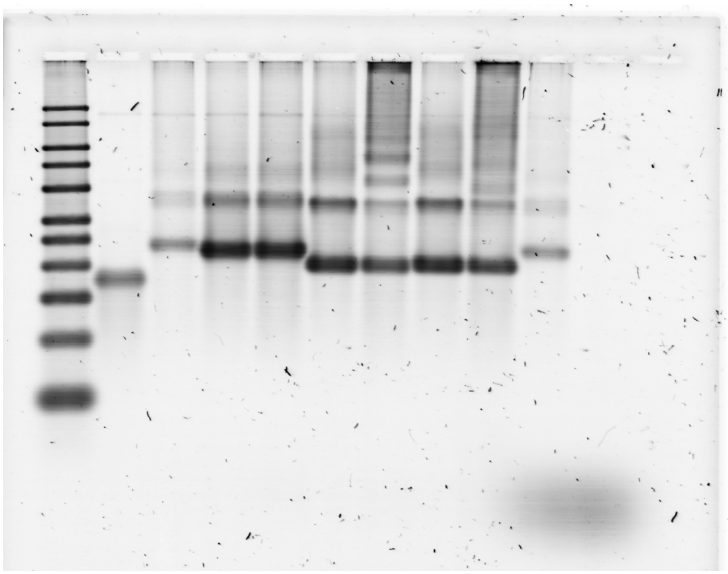

Fig. S9. Original gel images of Fig. SA without editing and annotations

We show these for transparency in data reportage. To obtain the images presented in Fig. SA, we applied the 'dust and scratches filter' in Photoshop to remove black specks. For the filter, we used a radius of 5 pixels and a threshold of 100.
The lanes are
1) 1 kb DNA ladder; 2) the m13mp18 plasmid; 3) R; 4) K_{NC}; 5) K_{NC}+R
6) K1; 7) K1+R; 8) K3; 9) K3+R; 10) R+anti strand; 11) anti strand; 12) MB strand

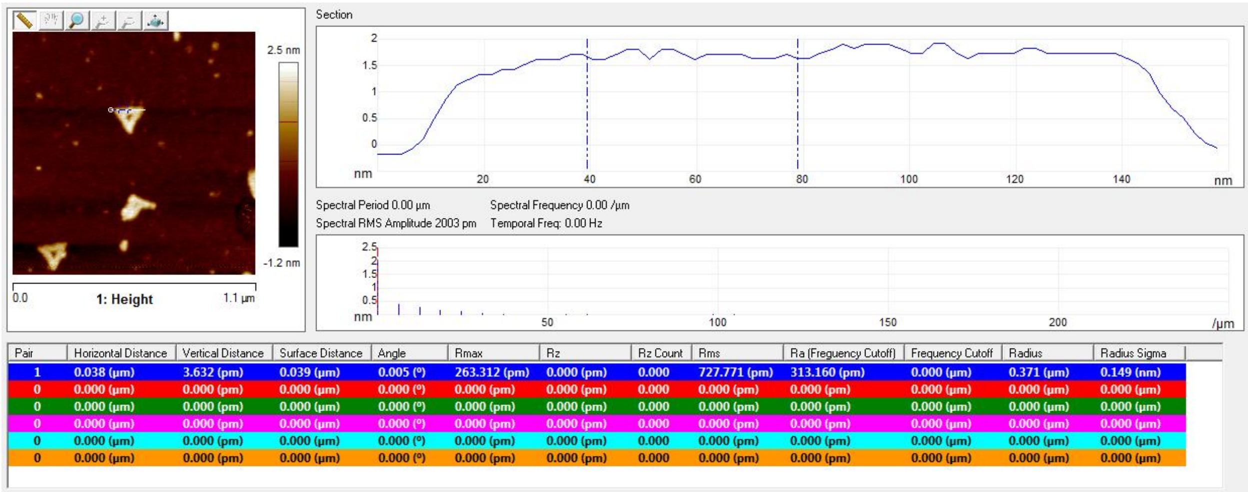

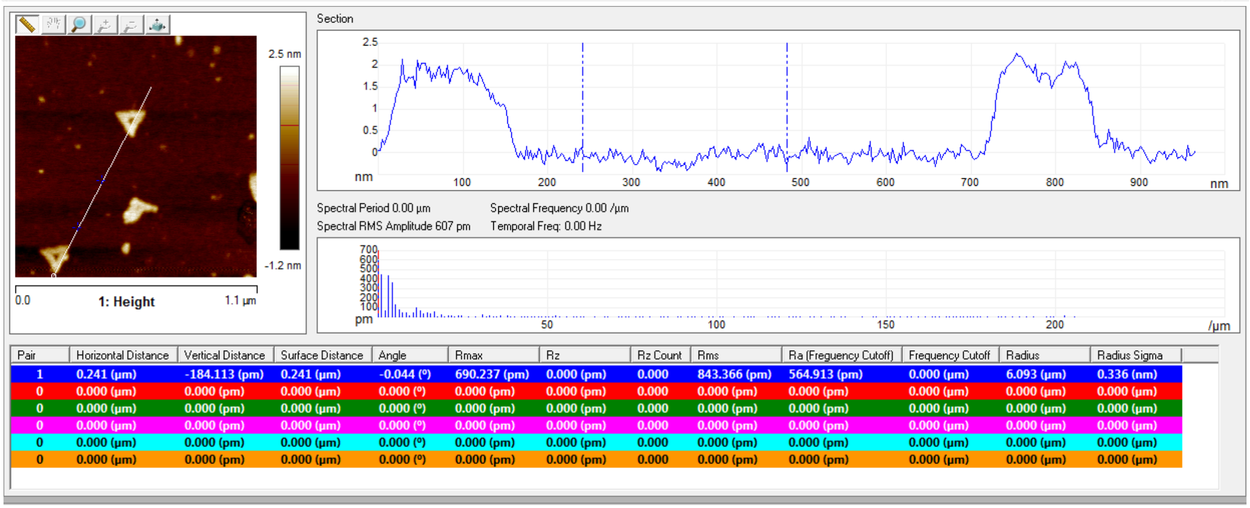

Fig S10. Cross section and distance AFM measurements of Receptor dimensions

We measured the dimensions of our origami tringles using Nanoscope Analysis software. Here we show representative snapshots of some of our receptor triangles, R, confirming 2 nm heights and 120 nm edge lengths.

Materials and Methods

Synthesis of DNA origami

We purchased all staple DNA Bio-RP-purified from Bioneer (Oakland, CA) with the exception of methylene-blue-modified strands, which were from from LGC Biosearch Technologies (Petaluma, CA), double-HPLC-purified. We obtained the m13mp18 plasmid from Guild Biosciences (Dublin, OH). Upon receiving all DNA we aliquoted it into DNA Lo-Bind Tubes from Eppendorf (Hauppauge, NY), and stored all DNA oligos, origami staple pools and origami assemblies in these tubes frozen at -20 °C.

We prepared the origami samples at 5 nM plasmid with a 4:1 staples-to-plasmid ratio (except for methylene-blue-containing strands, which were 12.5:1 per binding site), in HMg buffer supplemented with 1 mM Tris(2-carboxyethyl)phosphine hydrochloride (TCEP). We annealed these samples from 90 to 37 °C for 3 - 4 h in a water bath and then cooled them to 23 ºC and held them at this temperature for 20 min before use. Note: We reduced any disulfide bonds in DNA strands with TCEP during synthesis. After the synthesis, we removed all remaining TCEP from our origami solutions via multiple buffer exchanges. We observed that origami dimers form during synthesis whether we employed TCEP or not during their synthesis and that the presence of TCEP during storage did not cause more origami aggregation. Thus, the formation of origami dimers is likely not related to disulfide bonds.

We note that annealing the DNA origami with Magneisum concentrations > 11 mM, TCEP concentrations > 10 mM or at initial staple concentrations > 10 nM causes significant aggregation as seen by gel electrophoresis. If higher cation concentrations are required, either buffer exchange or additional Na/Mg can be added after annealing.

The 3'-C_6-PO_4-C_6-5'-thiol linker-modifed DNA was provided to us by Bioneer as a disulfide bound to hexanethiol. Reduction via TCEP produces the reduced species:

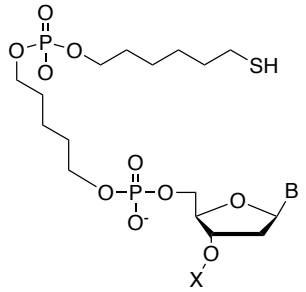

The methylene blue-modified nucleotide had the following structure as provided by LGC Biosearch Technologies:

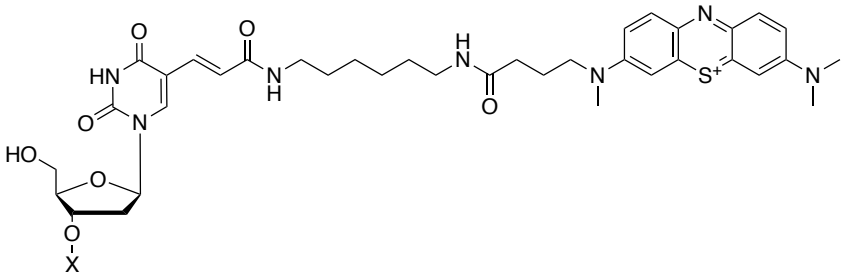

Origami Purification

For each 450 µL of crude 5nM origami solution, we used one Amicon Ultra-0.5mL Ultracel-100K MWCO filter device (Merck Millipore, Ireland) in a centrifuge at 25º C. We loaded the filter unit with 500 µL of HMg and spun it at 5k rcf, for 5 minutes. We then loaded 450 µL of sample and spun it at 5k rcf for 2 minutes. Then, we loaded 450 µL of buffer and spun the filter at 5k rcf for 2 minutes (3 times), discarding the eluate after each of the spins. Finally, we collected the sample by inverting the filter and spinning at 1k rcf for 2 minutes. This procedure gave us 50-75 µL of origami at 10-40 nM, with yields estimated by gel densitometry of 30-80%, most commonly ~20nM at ~60% yield. We note that, in our hands, excessive spin times, higher centrifugal forces or attempts to concentrate the samples further led to aggregation and/or lower yields.

For gel titration experiments, we identified the bands of interest via the intrinsic fluorescence of methylene blue, cut them out from agarose gels and recovered them as described by the Dietz Laboratory[6].

Fabrication of Au-coated Si wafers

We fabricated gold-coated silicon substrates via electron-beam evaporation. Briefly, we cleaned 100 mm diameter Si wafers (University Wafers, Boston, MA) by successively washing with acetone, 2-propanol and water. We then dried them for 5 minutes on a hotplate held at 100º C before cleaning them in a plasma oven (Technics PE-IIA System, PTB, Azusa, CA) for 30 seconds at 100 Watts and 0.30 Torr O_2. After plasma cleaning, we transferred the wafers to an electron-beam evaporation system (Temescal VES-2550, Livermore, CA). We first deposited a 200-Å-thick titanium bonding layer at a rate of 1 Å s^{-1}. Following this we deposited a 250-nm-thick gold layer at a rate of 1.5 Å s^{-1}. Finally, we diced the wafers into 1 cm^2 substrates using a dicing saw (ADT 7100, Tempe, AZ).

Functionalization of Au-coated Si wafers with DNA-origami

We immobilized DNA origami on freshly cleaned Au-coated substrates using thiol chemistry. Prior to functionalization, we removed residual organics from fabrication and dicing by washing the substrates first under a squirted-jet of acetone and second under a squirted jet of 2-propanol, for 10 s (**Fig. S11**). We then let the substrates fully dry under air. Once dry, we made an electrical connection to them using conductive copper tape (¼ inch, 3M, St. Paul, MN) and covered them with a section of a silicone gasket sheet (Press-To-Seal silicone isolator, GBL665208, Grace Bio-Labs, Bend, OR). The gasket was cut to contain just one hole in the center of the section, 2.0 mm in diameter, and was 2.0 mm thick (**Fig. S12**). We then placed these as-prepared substrates into a polytetrafluoroethylene (PTFE) electrochemical cell (CH Instruments, Austin, TX) in a configuration shown in **Fig. S13**. To prepare the substrates for monolayer and DNA deposition we electrochemically cleaned them by cycling their potential in 0.5 M H_2SO_4 from 0 V to 1.9 V vs a Ag/AgCl reference electrode (**Fig. S14**), 30 times, at a scanning rate of 1 V s^{-1}. This electrochemical treatment did not alter the surface roughness of the electrode as determined via contact mode AFM (**Fig. S1**). We employed a Multi-potentiostat (Model 1040C, CH Instruments, Austin, TX) and a platinum counter electrode for all the electrochemical procedures performed in this work. Immediately after electrochemically cleaning the substrates, we incubated them for 2-3 h in a 1 mM solution of 1,6-hexanedithiol (Sigma, USA) in PBS buffer. Following this incubation we washed

the substrates first with deionized water (18 MOhms, Millipore, Burlington, MA) and second with HMg, three times each. To evaluate the quality of the monolayer formed, 1ml of HMg was placed over the electrode, and we interrogated the substrates via square-wave voltammetry. We pulsed the potential from 0.0 to -0.45 V with square-wave step size of 1 mV, amplitude of 25 mV, and frequency of 60 Hz, 20 times. Functional substrates would typically present stable square-wave voltammograms with baseline currents below 100 nA (**Fig. S2**). Finally, we incubated these monolayer-coated substrates in 10 µL of 10-40 nM DNA origami dissolved in HMg for 2 h prior to further characterization. Note: This volume fully fills the gasket's hole. To prevent water evaporation during the incubation steps, we placed the substrates inside a hermetically-sealed plastic box with drops of water in the box to maintain a humid atmosphere. After incubation the gold surface and gasket were rinsed a minimum of 5 times with HMg, and electrochemical interrogation was carried out in 0.2-1mL of HMg.

Estimation of packing density

Our gasket has a 2 mm diameter circular hole (area = 3.15 mm^2). If we assume that the origami can only bind to the gold electrode by laying flat on its surface, the available flat area corresponds to ~ 3.15×10^{12} nm^2. The area covered by each origami triangle is 6,253 nm^2 (edge length ~120 nm). If close-packed in a 2d lattice on the gold surface, the maximum coverage would be 5.03×10^8 origami molecules per electrode. Each origami displays 12 methylene blue reporters, giving a maximum reporter density of 6.05×10^9 per electrode or ~2×10^7 per cm^2. (We would expect coverage to be lower than this because of origami-to-origami steric constraints on the surface.)

Experimentally, the packing densities on our electrodes translate to currents in the order of 10-80 nA. For reference, DNA aptamer-based electrodes, functionalized via the same procedure, would give µAs of current (at the same square-wave frequency) for surface densities[7] corresponding to 4×10^{12} reporters/cm^2. i.e. our total surface density of redox reporters is orders of magnitude lower than conventional DNA-based sensors.

Given the low density of the receptors on the surface, we are confident that surface-tethered origami are site-isolated and unable to crosslink. In this context, ‘crosslink’ means K3 or K1 triangles bind to the edges of two R molecules instead of forming a dimeric face-sharing structure. Ultimately, to demonstrate the absence of crosslinking with absolute certainty we would need to deposit the receptor from lower concentration stock solutions or for less time, as doing this would decrease the surface density of receptors and, thus, the probability of crosslinking upon binding. This experiment is not possible with our current design, however, because at the current surface densities the square-wave peak currents we obtain are already in the tens of nanoamperes. Further lowering the R surface density would only cause the current to drop too close to the noise floor to be able to measure any signaling from K3 or K1 binding. We note that *even if* there is limited crosslinking occurring, the sensor still discriminates between K3, K1 and K_{nc}.

In future work we will design receptors with higher signaling current (for example, by increasing the number of methylene blue reporters), which should allow us to run control dilution experiments to confirm the absence of crosslinking.

Electrochemical interrogation of DNA-origami-coated surfaces

We studied the electron transfer properties of DNA origami triangles via square-wave voltammetry, using the above-mentioned parameters. To determine the square-wave voltammetry frequencies that would optimally report changes in electron transfer kinetics we constructed Loveriç plots. For this, we interrogated DNA-origami-coated substrates with increasing square-wave frequencies and extracted peak currents from the voltammograms obtained. To measure time courses, we serially interrogated origami-functionalized substrates at different frequencies for up 2 h and extracted peak currents from the recorded voltammograms in real time via custom scripts written in Matlab language (See p 25 in this SI). **Note**: Tris-containing buffers, traditionally used in DNA origami study are inappropriate for electrochemical measurements because Tris is redox active with an E^0 of ~ -0.05 V vs Ag/AgCl.

Agarose gel studies.

We ran agarose gels (SeaKem GOLD Agarose) at 1-2% w/v and 23 ºC in 20mM HEPES (*p*H = 8.5) supplemented with 6 mM $MgCl_2$ hexahydrate (hereafter referred to as HMg). To prepare the gels, we heated a mixture of agarose and 20 mM HEPES in a 1200W microwave for 2.5 min or until boiling just started, followed by cooling in an ice bath to 60 °C. At this temperature we added $MgCl_2$ to reach a concentration of 6 mM. We poured the gel mixture onto the platform at 45 °C and cooled it for a minimum of 45 minutes prior to running. We ran the gels in OWL Buffer Puffer gel boxes. We first performed a prerun for ~50 V h, then loaded the samples and ran the gel for 400-600 V h, at ~ 30 V (2.2 V/cm). For gels studying the binding of orgiami, the voltage was set low enough to avoid ohmic heating of the gel (less than 2 ºC rise in temperature over the gel run). We loaded samples in HMg buffer containing 10% by volume loading buffer (50% glycerol in water, bromophenol blue 0.01g/ml). For the reference ladder we employed the Thermo Scientific™ GeneRuler™ 1kb DNA Ladder. We also used the plasmid m13mp18 (Guild biosciences) as an extra reference for the origami assembly.

Gels were imaged on a Typhoon 9500 molecular imaging system. Immediately after running, the gels were scanned with the 635 nm laser, LPR filter (cutoff below 665 nm) to visualize the intrinsic fluorescence of Methylene Blue containing bands. We then immediately stained the gels using Molecular Probes® by Life Technologies™ SYBR Gold nucleic acid gel stain (20 µL of 10,000X concentrate in 200 ml water) for 30 minutes and scanned with 473 nm laser, BPG1 filter (560-580 nm). Note: we prepared the staining solutions fresh every week as their efficacy decreases after this time.

Atomic force microscopy of origami on mica.

Triangle samples were deposited onto freshly cleaved mica for 2 – 60 s, washed with ~1 mL of filtered water, wicked and dried with a stream of compressed air from a can. Samples were visualized using a DI Nanoscope IIIa AFM, tapping mode, in air, using PPP-NCH tips (NanoAndMore).

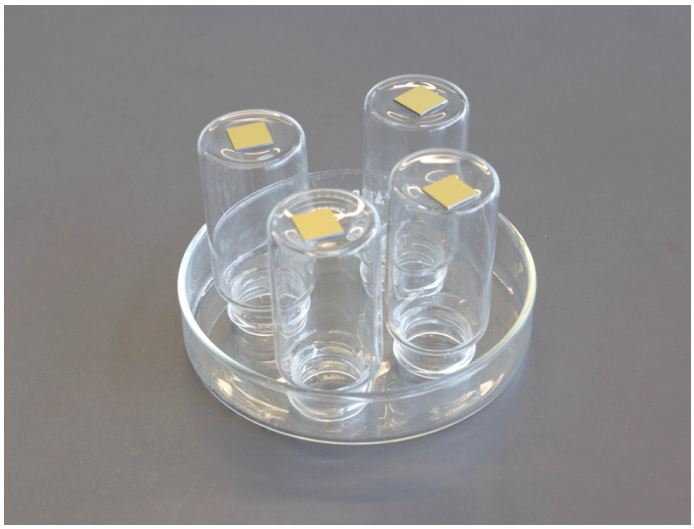

Fig. S11. Setup for solvent washing gold-coated wafers.

We placed freshly-diced gold-coated wafers on the base of inverted 30 mL glass vials. This configuration allowed any excess solvent to drip down the sides of the vials, preventing solvent stagnation. We squirted HPLC-grade acetone on top of each substrate continuously for 1 min, followed by washing with HPLC-grade 2-propanol for a further minute. After this, we let the substrates dry under air for about 5 min.

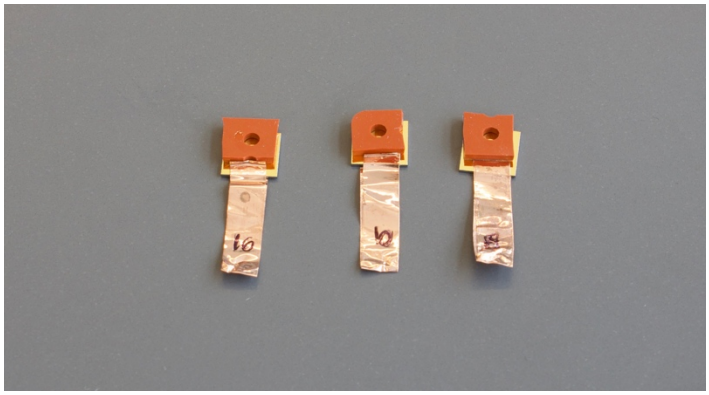

Fig. S12. Gold wafer modification into working electrodes of defined area.

After solvent cleaning, we made an electric contact to the gold-coated substrates using copper tape. After this we insulated the gold surfaces from the copper tape by placing an adhesive-coated and perforated silicone gasket on top of the substrates. We then modified the area of the electrode surrounded by the gasket as described in Materials and Methods.

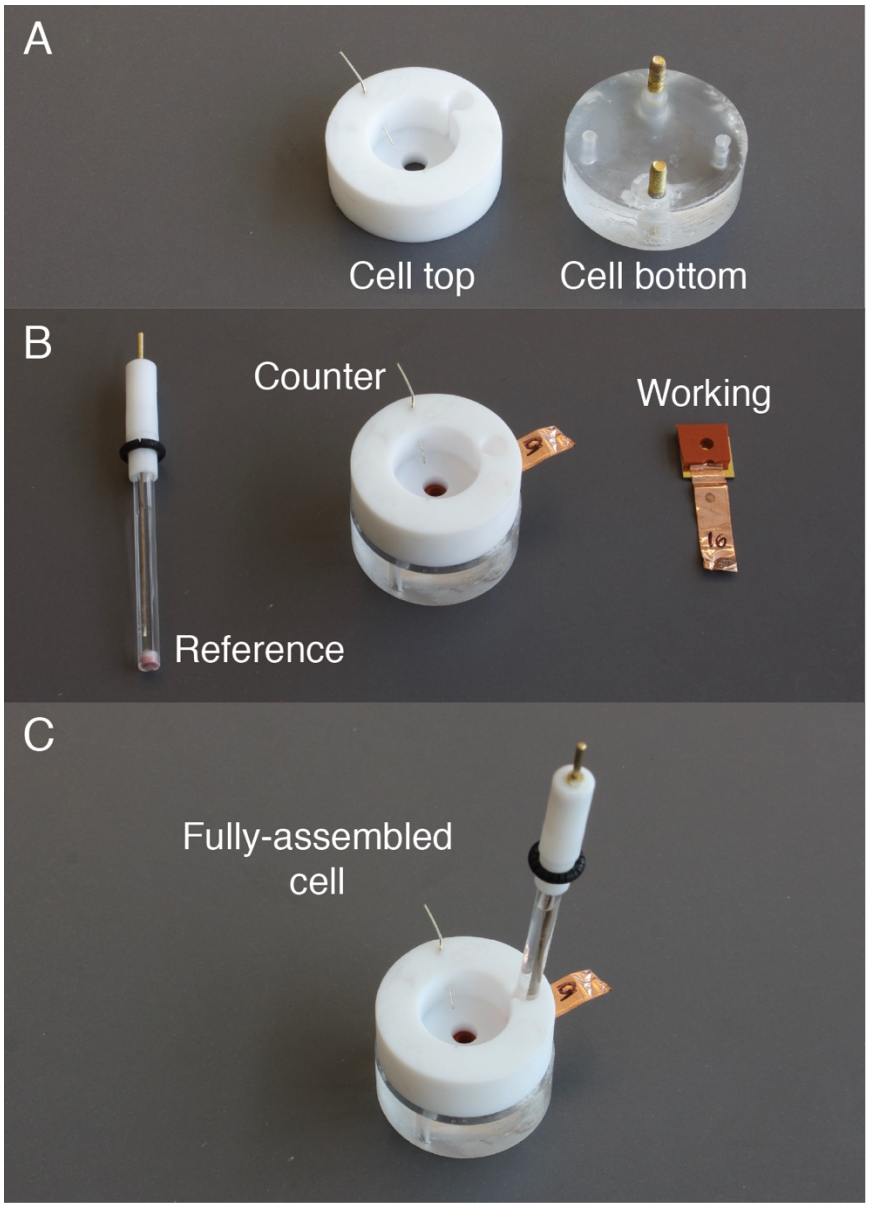

Fig. S13. Electrochemical cell assembly.

We used a cell design derived from scanning electrochemical microscopy. A-B) The white cell is made of poly(tetrafluoroethylene) and contains receptacles for reference and counter electrodes. It also has a 5 mm diameter window at the center to expose the substrate surface. The bottom part includes stainless steel screws for the final assembly. C) The origami-modified substrates are sandwiched inside the cell, with the gasket's hole aligned to the cell's window.

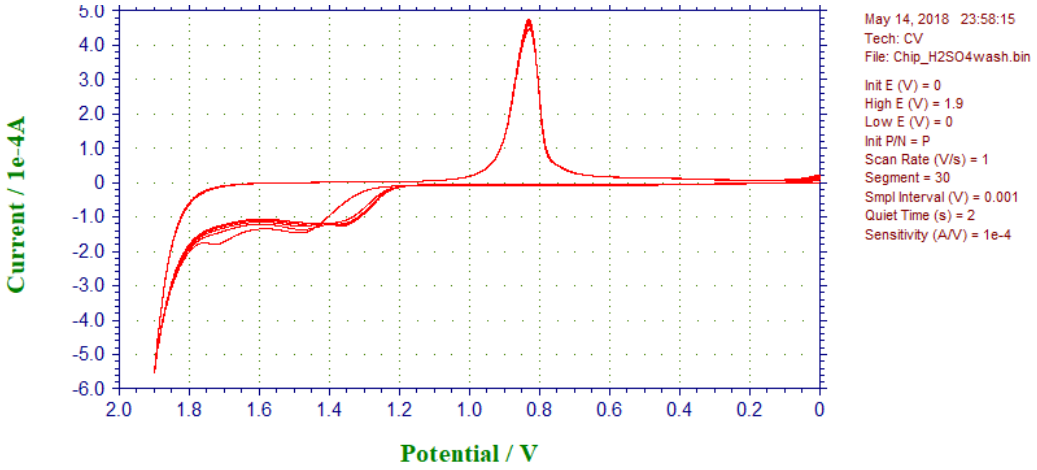

Fig. S14. Electrochemical cleaning of gold-coated substrates.

We cleaned the electrode surfaces via cyclic voltammetry in dilute sulfuric acid prior to functionalizing them with DNA origami[8]. By polarizing the substrates to 1.9 V vs Ag/AgCl in 0.5 M sulfuric acid we produced a monolayer of gold oxides, a fraction of which dissolves in these acidic conditions. We then reduced the gold oxides by sweeping back to 0.0 V, to obtain a cleaner, organics-free surface. We repeated this for 30 segments (15 cycles), until the voltammograms showed reproducible behavior. By doing this, we observed a reorganization of the surface as evidenced by changes in the shape of the voltammogram, until a steady voltammogram was obtained.

OxDNA: Molecular Dynamics Configuration

OxDNA has been widely used to model DNA origami structures[9-11], including multi-component dynamic devices[12]. Here we followed a similar simulation workflow as previously presented[13].

The three DNA origami designs (R, K1, and K3) were first individually converted from cadnano designs (.json files) to coarse-grained oxDNA models (https://dna.physics.ox.ac.uk). We then applied rigid-body transformations on each of the trapezoid components to assemble them into the triangle configuration.

Each of the triangle structures (R, K1, and K3) was relaxed as previously described[13]. The R structure was simulated individually for 3e8 steps, corresponding to ~1500 μs, with 6 anchor forces located at the sites where strands protrude to attach to the electrode surface (green spheres in Figure S15).

To form the R+K1 and R+K3 complexes, we first ran short simulations of each structure, 1e7 steps or ~=50 μs, with the same anchoring sites to obtain realistic initial configurations for binding. To bind K1 and K3 with R, we took the configurations from the short time simulations, and specified the sequences on the 5 binding sites on each edge to T40 and A40 (e.g. purple strands in figure S15 (slide 3)), and included mutual traps (attractive forces) until the T40 and A40 strands were hybridized together. Once the structures were bound together, we performed simulations for 3e8 steps with anchoring forces only applied to the R anchor sites.

Fig. S15: OxDNA simulation: Average configuration of the R structure.

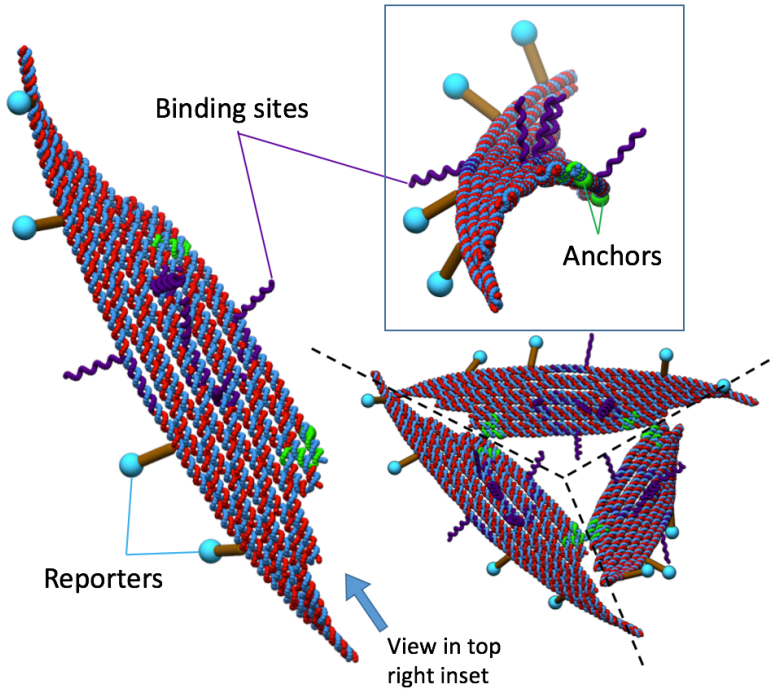

The triangle receptor (R) structure was simulated in oxDNA. We determined the average configuration of the structure by averaging the location of individual bases on the backbone over all 1500 frames of the simulation. The binding sites for K1 and K3 are illustrated in purple, and the redox label sites (reporters) are illustrated as cyan spheres. The green sites show where the structure were anchored, which are the sites that contain protruding strands that attach to the surface. The bottom right shows the full structure, and the left side zoom in illustrates a single trapezoid panel. Furthermore, the top right inset illustrates a side view of the trapezoid panel. We observed the structures converged to a configuration with global twist on three edges due, which is a common feature of square lattice DNA origami structures. The averaged configuration illustrated here was used as the reference from to calculate RMSD values, unless otherwise noted.

Fig. S16: OxDNA simulation: Non-averaged traces compared to 20-point-averaged traces

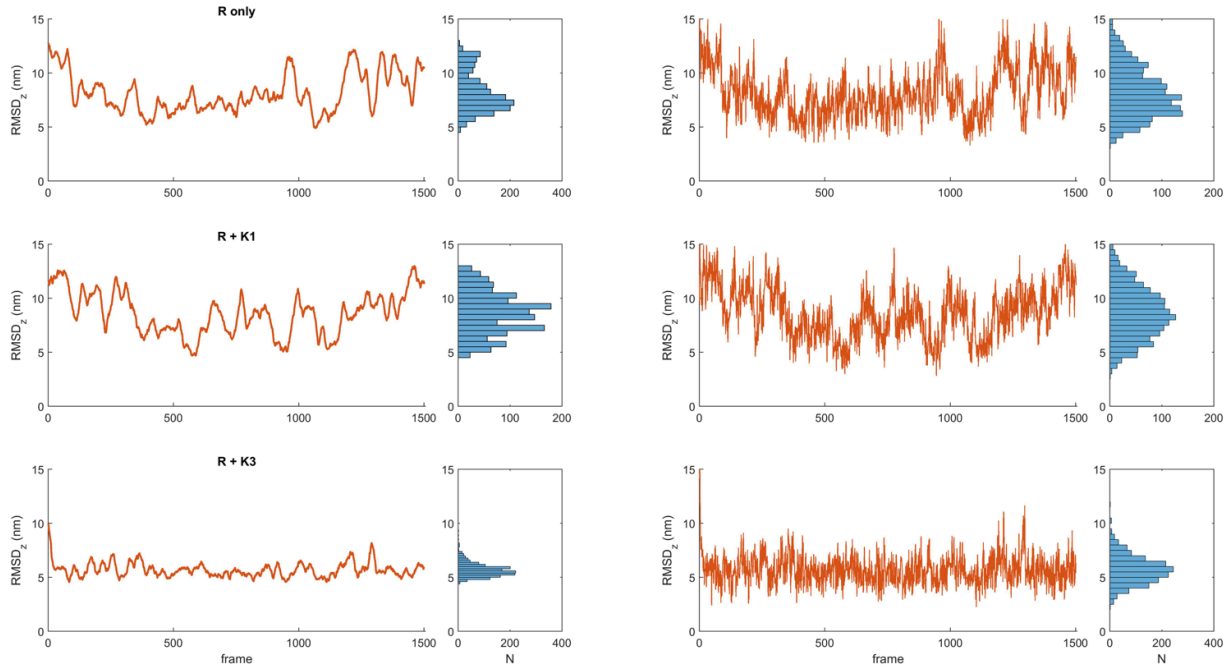

The averaging filters out very fast fluctuations, which are likely local fluctuations of the duplex strands containing the redox labels. Removing these fast fluctuations also removes the tails of the RMSD distributions depicted in the histograms. However, the trend of reduced RMSD is still clear, and the average RMSD value is the same for both N-averaged or raw data.

Fig. S17: OxDNA simulation: Magnitude of RMSD fluctuations varies depending on reference configuration – overall trends maintained

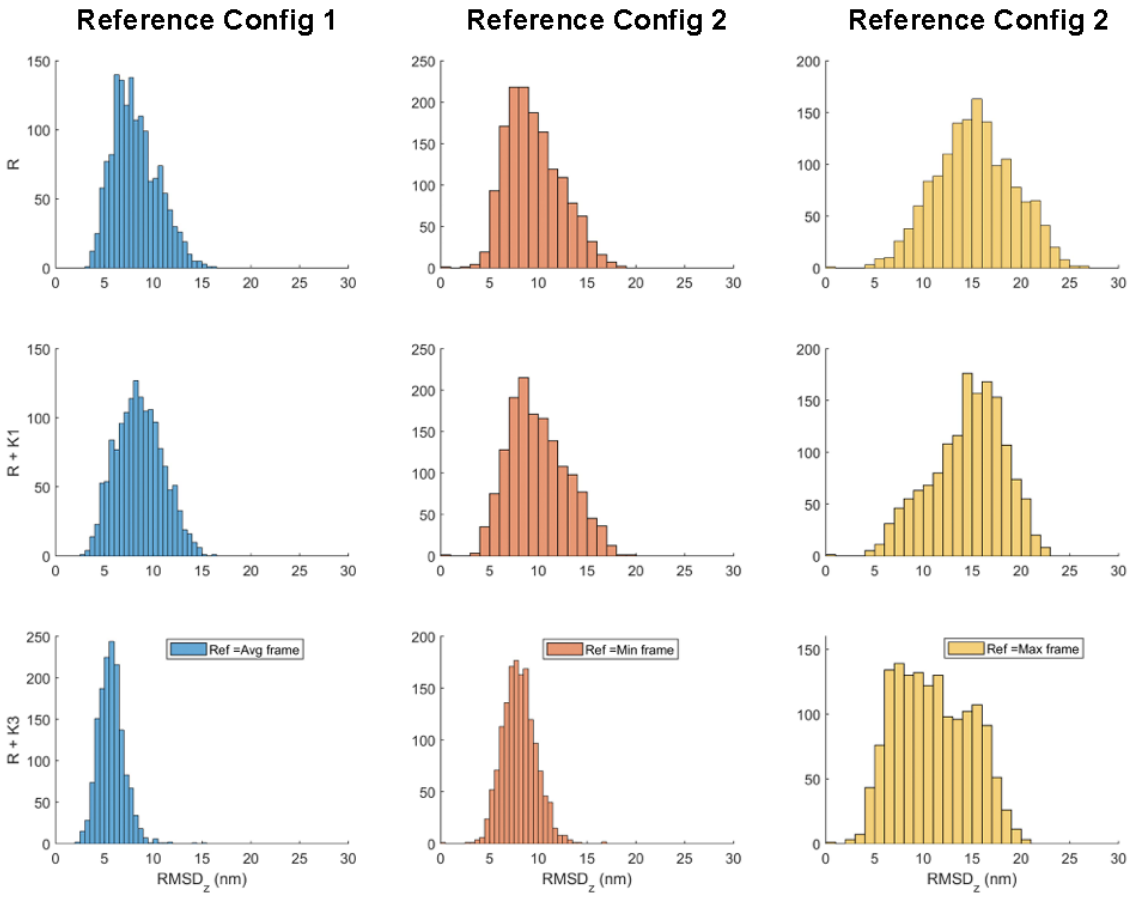

To improve model universality, reference configurations for the receptor were chosen at minimum, mean and maximum deformations from the mean receptor structure. In all cases the reduction in RMSD upon binding R+K3 is still clear.

Fig. S18: OxDNA Simulation: Thermal fluctuations of complexes in all 3 dimensions

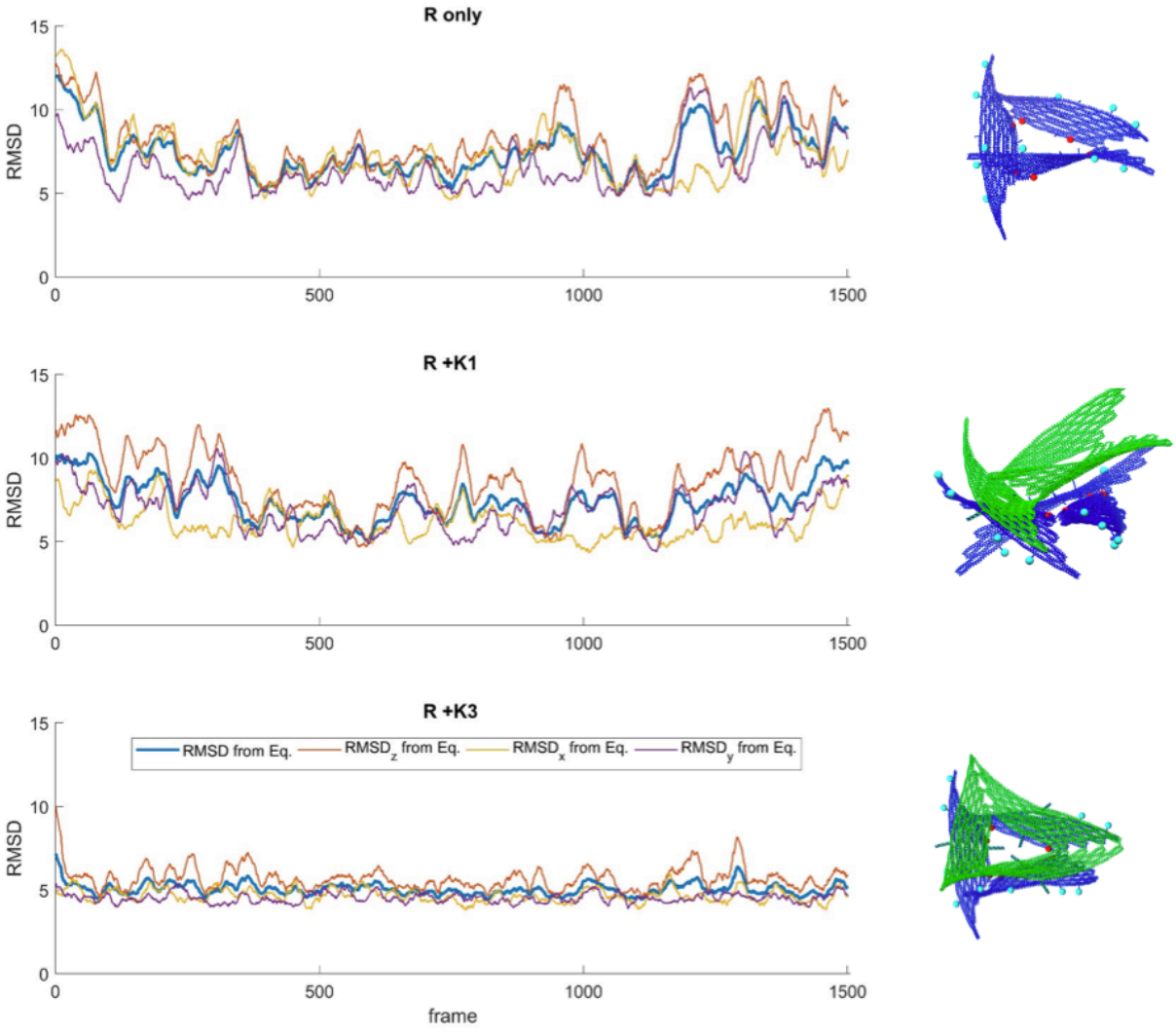

While the coordinate that determines distance from (or collisions with) the electrode surface is the z-direction, here we illustrate RMSD values calculated in all 3 directions relative to the averaged configuration. The RMSD values in all directions are similar to the R structure by itself upon binding R+K1, while binding of R+K3 causes a significant decrease of RMSD in all three directions.

Matlab™ Script for Real-Time Analysis of Square-wave Voltammograms

To use script, copy-paste onto Matlab's editor.

```
%%%%%%%%%%%%%%%%%%%%%%%%%%%%%%%%%%%%%%%%%%%%%%%%%%%%%%%%%%%%%%%%%%%%%%%%%%%%
%
% Program for real-time analysis of square-wave voltammograms
% Created by Netz Arroyo on April 2018
%
%%%%%%%%%%%%%%%%%%%%%%%%%%%%%%%%%%%%%%%%%%%%%%%%%%%%%%%%%%%%%%%%%%%%%%%%%%%%
%%
%% Clear workspace
%%
%%%%%%%%%%%%%%%%%%%%%%%%%%%%%%%%%%%%%%%%%%%%%%%%%%%%%%%%%%%%%%%%%%%%%%%%%%%%
fclose('all');
clear
clc
close all
%%%%%%%%%%%%%%%%%%%%%%%%%%%%%%%%%%%%%%%%%%%%%%%%%%%%%%%%%%%%%%%%%%%%%%%%%%%%
%%
%% Setting up variables
%%
%%%%%%%%%%%%%%%%%%%%%%%%%%%%%%%%%%%%%%%%%%%%%%%%%%%%%%%%%%%%%%%%%%%%%%%%%%%%
frequencies = {30 60 100 200};     % Add frequencies to be analyzed
setpointNorm = 1;            % Point to normalize peak heights to
points_smooth = 5;           % Points included in rolling average
maxIter = 916;              % Number of experiments
ystart = 5;                % Points discarded at beginning of voltammogram
yend = 5;                 % Points discarded at end of voltammogram
fitstart = 5;               % Points discarded at the beginning for polynomial
fit
fitend = 5;                % Points discarded at the end for polynomial fit
experimentName = 'Name_';        % Name for txt files exported
folderName = '/Users/Username/data';  % Path to files
Npolynomial = 15;            % Degree of polynomial fit
unit_x = 'Time (min)';         % Label for x axis
unit_y = ['m';'u';'n'];         % Scale for numbers in y axis
Factorconvert = 6;           % Order of magnitude of the concentration
[1=M,3=mM,6=uM,9=nM]

%%%%%%%%%%%%%%%%%%%%%%%%%%%%%%%%%%%%%%%%%%%%%%%%%%%%%%%%%%%%%%%%%%%%%%%%%%%%
%%
%% Pre-allocation of variables
%%
%%%%%%%%%%%%%%%%%%%%%%%%%%%%%%%%%%%%%%%%%%%%%%%%%%%%%%%%%%%%%%%%%%%%%%%%%%%%
pastConcentration = zeros(maxIter,1);
diff = cell(1,length(frequencies));
diff_norm = cell(1,length(frequencies));
for ii = 1:length(frequencies) % loop through every frequency
  diff[8] = ones(maxIter,1);
  diff_norm[8] = ones(maxIter,1);
end
%%%%%%%%%%%%%%%%%%%%%%%%%%%%%%%%%%%%%%%%%%%%%%%%%%%%%%%%%%%%%%%%%%%%%%%%%%%%
%%
%% Reading files
%%
%%%%%%%%%%%%%%%%%%%%%%%%%%%%%%%%%%%%%%%%%%%%%%%%%%%%%%%%%%%%%%%%%%%%%%%%%%%%
figure()
```

```
iter = 1; % first titration point
while iter <= maxIter % Loop through titration points
  for ii = 1:length(frequencies) % Loop through all frequencies
    freq = frequencies(ii);

    %%%%%%%%%%%%%%%%%% Name of your files %%%%%%%%%%%%%%%%%%%%%%%%%
    myfilename =
strcat(folderName,'/','6electrode_',num2str(freq),'Hz__',num2str(iter),'.txt'
);
    % In this example: "/Users/Username/data/6electrode_10Hz__1.txt"
    %%%%%%%%%%%%%%%%%%%%%%%%%%%%%%%%%%%%%%%%%%%%%%%%%%%%%%%%%%%%%%%%

    fid = fopen(myfilename,'r'); % open file (read only)
    if fid==-1 % keep trying until the file is found
      while fid==-1
        tic
        fid = fopen(myfilename,'r'); % open file (read only)
        if toc > 300 % 5 minutes spent on searchinng for file
          error(['Timeout in search for ', myfilename]); % timeout error
        end
      end
    end % file has been found
    T = readtable(myfilename,'FileType','text','HeaderLines',1); % read in
data
    data_y = T{ystart:end-yend,{'Var2'}};  % Potential/V
    data_x = T{ystart:end-yend,{'Var1'}};  % Current/A
    fclose('all'); % close files opened

%%%%%%%%%%%%%%%%%%%%%%%%%%%%%%%%%%%%%%%%%%%%%%%%%%%%%%%%%%%%%%%%%%%%%%%
    %%
    %% Smoothing function and polynomial fitting
    %%

%%%%%%%%%%%%%%%%%%%%%%%%%%%%%%%%%%%%%%%%%%%%%%%%%%%%%%%%%%%%%%%%%%%%%%%
    warning('off', 'MATLAB:polyfit:RepeatedPointsOrRescale');
    Y_smooth = smooth(data_y,points_smooth); % moving average of data points,
decided by points_smooth
    P = polyfit(data_x(fitstart:end-fitend),Y_smooth(fitstart:end-
fitend),Npolynomial); % P is a row vector of coefficients.
    Y = polyval(P,data_x(fitstart:end-fitend));


%%%%%%%%%%%%%%%%%%%%%%%%%%%%%%%%%%%%%%%%%%%%%%%%%%%%%%%%%%%%%%%%%%%%%%%
    %%
    %% Plot data, smoothed data and polynomial fits
    %%

%%%%%%%%%%%%%%%%%%%%%%%%%%%%%%%%%%%%%%%%%%%%%%%%%%%%%%%%%%%%%%%%%%%%%%%
    subplot(2,length(frequencies),ii,'replace')
%     plot(data_x,data_y./1e-6,'k.','MarkerSize',20); % RAW VOLTAMMOGRAMS
    xlim([min(data_x) max(data_x)]);
    ylim([(0.5 * max(data_y./1e-6)) (1.1 * max(data_y./1e-6))]);
    hold on
    plot(data_x,Y_smooth./1e-6,'b.','MarkerSize',15); % SMOOTHED
VOLTAMMOGRAMS
    plot(data_x(fitstart:end-fitend),Y./1e-6,'r-'); % POLYNOMIAL OVER
SMOOTHED VOLTAMMOGRAMS
    ylabel('Current / μA','fontweight','bold');
```

```
    xlabel('Potential / V','fontweight','bold');
    title([num2str(frequencies(8)), ' Hz']);
    hold off
    ax = gca;
    ax.YAxis.TickLabelFormat = '%,.1f';


%%%%%%%%%%%%%%%%%%%%%%%%%%%%%%%%%%%%%%%%%%%%%%%%%%%%%%%%%%%%%%%%%%%%%%%%%%%%%%%
    %%
    %% Determine peak heights
    %%

%%%%%%%%%%%%%%%%%%%%%%%%%%%%%%%%%%%%%%%%%%%%%%%%%%%%%%%%%%%%%%%%%%%%%%%%%%%%%%%
    j = length(Y); % j is the index in the data (number of data points)
    first_valley = min(Y(1:floor(j/2)));
    second_valley = min(Y(ceil(j/2):end));
    peak = max(Y);
    % compute difference between peak and higher valley:
    diff(8)(iter) = (peak - max(first_valley,second_valley));
    diff_norm(8)(iter) = diff(8)(iter)/diff(8)(1);
    Inorm = (cat(2,(1:iter)',diff_norm(8)(1:iter)));
    Iraw = (cat(2,(1:iter)',diff(8)(1:iter)));
    % save data to files
    fname=sprintf('%s_Inorm_%d_HZ.txt',experimentName,freq);
    save(fname,'Inorm','-ascii','-tabs');
    fname=sprintf('%s_Iraw_%d_HZ.txt',experimentName,freq);
    save(fname,'Iraw','-ascii','-tabs');


%%%%%%%%%%%%%%%%%%%%%%%%%%%%%%%%%%%%%%%%%%%%%%%%%%%%%%%%%%%%%%%%%%%%%%%%%%%%%%%
    %%
    %% Plot peak heights
    %%
%%%%%%%%%%%%%%%%%%%%%%%%%%%%%%%%%%%%%%%%%%%%%%%%%%%%%%%%%%%%%%%%%%%%%%%%%%%%%%%
    subplot(2,length(frequencies),ii+length(frequencies),'replace')
    if ii == 1
      plot(1:iter,diff_norm(8)(1:iter) +
baselineslope*(1:iter)','b.','MarkerSize',10); % NORMALIZED CURRENTS
    else
      plot(1:iter,diff_norm(8)(1:iter),'b.','MarkerSize',10); % NORMALIZED
CURRENTS
    end
    xlabel('Voltamogram #','fontweight','bold');
    ylabel('Normalized Peak Current','fontweight','bold');
    ylim([0, 3]);
    drawnow
  end % end frequency loop
  disp(iter)
  iter = iter + 1; % move on to next point
end % end while iter
%%%%%%%%%%%%%%%%%%%%%%%%%%%%%%%%%%%%%%%%%%%%%%%%%%%%%%%%%%%%%%%%%%%%%%%%%%%%%%%
%% Program ends here
%%%%%%%%%%%%%%%%%%%%%%%%%%%%%%%%%%%%%%%%%%%%%%%%%%%%%%%%%%%%%%%%%%%%%%%%%%%%%%%
```

Strand pool combinations for Receptors and Targets

	Receptor (R)	K_{NC}	K3	K1
General Stock A	+	+	-	-
General Stock B	-	-	+	+
Loops	-	-	+	-
Down-Thiol	+	-	-	-
Down-Blunt	-	+	+	+
Side-TGA-MB	+	-	-	-
Side-Blunt	-	+	+	+
Up-A40x15	+	+	-	-
Up-T40x15	-	-	+	-
Up-T40x5	-	-	-	+

	$R_{(NO-SH)}$	$R_{(MB-UP)}$
General Stock A	+	+
General Stock B	-	-
Loops	-	-
Down-Thiol	-	+
Down-Blunt	+	-
Side-TGA-MB	+	-
Side-Blunt	-	-
Up-A40x15	+	-
Up-TGAx15	-	+
Side-A40	-	+

For R, $R_{(NO-SH)}$ and $R_{(MB-UP)}$ add "MB strand".

Strand pool sequences for Receptors and Targets

Down-Thiol	A9	*GATAAGTGCCGTCGAGCTGAAACATGAAAGTATACAGGAG
***=thiol anchor**	A38	*AAAACAAAATTAATTAAATGGAAACAGTACATTAGTGAAT
	B9	*AGAAAAGCCCCAAAAAGAGTCTGGAGCAAACAATCACCAT
	B38	*CCTCAGAACCGCCACCCAAGCCCAATAGGAACGTAAATGA
	C9	*CCTGATTGCTTTGAATTGCGTAGATTTTCAGGCATCAATA
	C38	*GCTCATTTTTTAACCAGCCTTCCTGTAGCCAGGCATCTGC
	A5	TTTGATGATTAAGAGGCTGAGACTTGCTCAGTACCAGGCG
	A42	AGAGTCAAAAATCAATATATGTGATGAAACAAACATCAAG
	B5	ACAGTCAAAGAGAATCGATGAACGACCCCGGTTGATAATC
	B42	AGACGTTACCATGTACCGTAACACCCCTCAGAACCGCCAC
	C5	TGGCAATTTTTAACGTCAGATGAAAACAATAACGGATTCG
	C42	GTAACCGTCTTTCATCAACATTAAAATTTTTGTTAAATCA
Down-Blunt	A9	GATAAGTGCCGTCGAGCTGAAACATGAAAGTATACAGGAG
	A38	AAAACAAAATTAATTAAATGGAAACAGTACATTAGTGAAT
	B9	AGAAAAGCCCCAAAAAGAGTCTGGAGCAAACAATCACCAT
	B38	CCTCAGAACCGCCACCCAAGCCCAATAGGAACGTAAATGA
	C9	CCTGATTGCTTTGAATTGCGTAGATTTTCAGGCATCAATA
	C38	GCTCATTTTTTAACCAGCCTTCCTGTAGCCAGGCATCTGC
	A5	TTTGATGATTAAGAGGCTGAGACTTGCTCAGTACCAGGCG
	A42	AGAGTCAAAAATCAATATATGTGATGAAACAAACATCAAG
	B5	ACAGTCAAAGAGAATCGATGAACGACCCCGGTTGATAATC
	B42	AGACGTTACCATGTACCGTAACACCCCTCAGAACCGCCAC
	C5	TGGCAATTTTTAACGTCAGATGAAAACAATAACGGATTCG
	C42	GTAACCGTCTTTCATCAACATTAAAATTTTTGTTAAATCA
Side-TGA-MB	A61	GCGCCTGTTATTCTAAGAACGCGATTCCAGAGCCTAATTTGCCAGTTACAATTTTGATGATGATGATGATGATGA
	A49	AGCATGTATTTCATCGTAGGAATCAAACGATTTTTTGTTTAACGTCAAAAATTTTGATGATGATGATGATGATGA
	A20	TTGACGGAAATACATACATAAAGGGCGCTAATATCAGAGAGATAACCCACATTTTGATGATGATGATGATGATGA
	A30	GAGCCAGCGAATACCCAAAAGAACATGAAATAGCAATAGCTATCTTACCGATTTTGATGATGATGATGATGATGA
	B61	AAAACACTTAATCTTGACAAGAACTTAATCATTGTGAATTACCTTATGCGATTTTGATGATGATGATGATGATGA

	B49	TATCATCGTTGAAAGAGGACAGATGGAAGAAAAATCTACGTTAATAAAACGTTTTG ATGATGATGATGATGATGA
	B20	TAATTGCTTTACCCTGACTATTATGAGGCATAGTAAGAGCAACACTATCATTTTTG ATGATGATGATGATGATGA
	B30	TGCTGTAGATCCCCCTCAAATGCTGCGAGAGGCTTTTGCAAAAGAAGTTTTTTTT GATGATGATGATGATGATGA
	C61	TTCCAGTCCTTATAAATCAAAAGAGAACCATCACCCAAATCAAGTTTTTTGTTTTGA TGATGATGATGATGATGA
	C49	GTTTGCGTCACGCTGGTTTGCCCCAAGGGAGCCCCCGATTTAGAGCTTGACTTTT GATGATGATGATGATGATGA
	C20	GAATACGTAACAGGAAAAACGCTCCTAAACAGGAGGCCGATTAAAGGGATTTTTT GATGATGATGATGATGATGA
	C30	TAAAACATTAGAAGAACTCAAACTTTTTATAATCAGTGAGGCCACCGAGTATTTTG ATGATGATGATGATGATGA
	A59	AATAATAGAAGGCTTATCCGGTTATCAAC
	A45	TGAAAAGCAAGCCGTTTTTATGAAACCAA
	A23	AGAATGTTAGCAAACGTAGAAAATTATTC
	A31	AGCCCAAACGCAATAATAACGAAAATCACCAG
	B59	TTTTATGACCTTCATCAAGAGCATCTTTG
	B45	AACTAACCGAACTGACCAACTCCTGATAA
	B23	AACCCATCAAAAATCAGGTCTCCTTTTGA
	B31	GCCAGCATAAATATTCATTGACTCAACATGTT
	C59	GGGTCGAAATCGGCAAAATCCGGGAAACC
	C45	GGGGAGTTGCAGCAAGCGGTCATTGGGCG
	C23	TTAGATACCGCCAGCCATTGCGGCACAGA
	C31	AAAGAACATCACTTGCCTGAGCGCCATTAAAA
Side-Blunt	A61	GCGCCTGTTATTCTAAGAACGCGATTCCAGAGCCTAATTT
	A49	AGCATGTATTTCATCGTAGGAATCAAACGATTTTTTGTTT
	A20	TTGACGGAAATACATACATAAAGGGCGCTAATATCAGAGA
	A30	GAGCCAGCGAATACCCAAAAGAACATGAAATAGCAATAGC
	B61	AAAACACTTAATCTTGACAAGAACTTAATCATTGTGAATT
	B49	TATCATCGTTGAAAGAGGACAGATGGAAGAAAAATCTACG
	B20	TAATTGCTTTACCCTGACTATTATGAGGCATAGTAAGAGC
	B30	TGCTGTAGATCCCCCTCAAATGCTGCGAGAGGCTTTTGCA
	C61	TTCCAGTCCTTATAAATCAAAAGAGAACCATCACCCAAAT
	C49	GTTTGCGTCACGCTGGTTTGCCCCAAGGGAGCCCCCGATT
	C20	GAATACGTAACAGGAAAAACGCTCCTAAACAGGAGGCCGA
	C30	TAAAACATTAGAAGAACTCAAACTTTTTATAATCAGTGAG
	A59	GCCAGTTACAAAATAATAGAAGGCTTATCCGGTTATCAAC
	A45	AACGTCAAAAATGAAAAGCAAGCCGTTTTTATGAAACCAA
	A23	GATAACCCACAAGAATGTTAGCAAACGTAGAAAATTATTC
	A31	TATCTTACCGAAGCCCAAACGCAATAATAACGAAAATCACCAG
	B59	ACCTTATGCGATTTTATGACCTTCATCAAGAGCATCTTTG

	B45	TTAATAAAACGAACTAACCGAACTGACCAACTCCTGATAA
	B23	AACACTATCATAACCCATCAAAAATCAGGTCTCCTTTTGA
	B31	AAAGAAGTTTTGCCAGCATAAATATTCATTGACTCAACATGTT
	C59	CAAGTTTTTTGGGGTCGAAATCGGCAAAATCCGGGAAACC
	C45	TAGAGCTTGACGGGGAGTTGCAGCAAGCGGTCATTGGGCG
	C23	TTAAAGGGATTTTAGATACCGCCAGCCATTGCGGCACAGA
	C31	GCCACCGAGTAAAAGAACATCACTTGCCTGAGCGCCATTAAAA
Up-A40x15	A10	TGTACTGGAAATCCTCATTAAAGCAGAGCCACAAAAAAAAAAAAAAAAAAAAAAAAAAAAAAAAA
	A33	CCTTTTTTCATTTAACAATTTCATAGGATTAGAAAAAAAAAAAAAAAAAAAAAAAAAAAAAAAAA
	A35	AGTATAAAATATGCGTTATACAAAGCCATCTTAAAAAAAAAAAAAAAAAAAAAAAAAAAAAAAAA
	A37	AGAGAATAACATAAAAACAGGGAAGCGCATTAAAAAAAAAAAAAAAAAAAAAAAAAAAAAAAAA
	A39	TTATCAAACCGGCTTAGGTTGGGTAAGCCTGTAAAAAAAAAAAAAAAAAAAAAAAAAAAAAAAA
	B10	CAATATGACCCTCATATATTTTAAAGCATTAAAAAAAAAAAAAAAAAAAAAAAAAAAAAAAAAA
	B33	AGGGATAGCTCAGAGCCACCACCCCATGTCAAAAAAAAAAAAAAAAAAAAAAAAAAAAAAAAAA
	B35	GCCGCTTTGCTGAGGCTTGCAGGGGAAAAGGTAAAAAAAAAAAAAAAAAAAAAAAAAAAAAAAA
	B37	ACAGGTAGAAAGATTCATCAGTTGAGATTTAGAAAAAAAAAAAAAAAAAAAAAAAAAAAAAAAAA
	B39	ATTTTCTGTCAGCGGAGTGAGAATACCGATATAAAAAAAAAAAAAAAAAAAAAAAAAAAAAAAAA
	C10	TAATCCTGATTATCATTTTGCGGAGAGGAAGGAAAAAAAAAAAAAAAAAAAAAAAAAAAAAAAAA
	C33	CGCGTCTGATAGGAACGCCATCAACTTTTACAAAAAAAAAAAAAAAAAAAAAAAAAAAAAAAAAA
	C35	CTCTAGAGCAAGCTTGCATGCCTGGTCAGTTGAAAAAAAAAAAAAAAAAAAAAAAAAAAAAAAAA
	C37	CGAGAAAGGAAGGGAAGCGTACTATGGTTGCTAAAAAAAAAAAAAAAAAAAAAAAAAAAAAAAAA
	C39	CAGTTTGACGCACTCCAGCCAGCTAAACGACGAAAAAAAAAAAAAAAAAAAAAAAAAAAAAAAAA
Up-T40x15	A1	TTTTTTTTTTTTTTTTTTTTTTTTTTTTTTTTTTTTTTTTTTTTCGGGGTTTCCTCAAGAGAA GGATTTTGAATTA
	A3	TTTTTTTTTTTTTTTTTTTTTTTTTTTTTTTTTTTTTTTTTTTTTTTTCATAATCCCCTTATTAGC GTTTTTCTTACC
	A8	TTTTTTTTTTTTTTTTTTTTTTTTTTTTTTTTTTTTTTTTTTTTTTTTGACGGGAGAATTAACTCGG AATAAGTTTATTTCCAGCGCC
	A11	TTTTTTTTTTTTTTTTTTTTTTTTTTTTTTTTTTTTTTTTTTTTTTTTCACCGGAAAGCGCGTTTTC ATCGGAAGGGCGA
	A40	TTTTTTTTTTTTTTTTTTTTTTTTTTTTTTTTTTTTTTTTTTTTTTTTAGTATCGCCAACGCTCAA CAGTCGGCTGTC
	B1	TTTTTTTTTTTTTTTTTTTTTTTTTTTTTTTTTTTTTTTTTTTTTTTTCATATGTGTAATCGTAAAA CTAGTCATTTTC

	B3	TTTTTTTTTTTTTTTTTTTTTTTTTTTTTTTTTTTTTTTTTTGGCATCAAATTTGGGGCGC GAGCTAGTTAAAG
	B8	TTTTTTTTTTTTTTTTTTTTTTTTTTTTTTTTTTTTTTTTTTGAATACCACATTCAACTTAA GAGGAAGCCCGATCAAAGCG
	B11	TTTTTTTTTTTTTTTTTTTTTTTTTTTTTTTTTTTTTTTTTTCATCCAATAAATGGTCAATA ACCTCGGAAGCA
	B40	TTTTTTTTTTTTTTTTTTTTTTTTTTTTTTTTTTTTTTTTTTATTCGGTCTGCGGGATCGT CACCCGAAATCCG
	C1	TTTTTTTTTTTTTTTTTTTTTTTTTTTTTTTTTTTTTTTTTTCGGGAGATATACAGTAACA GTACAAATAATT
	C3	TTTTTTTTTTTTTTTTTTTTTTTTTTTTTTTTTTTTTTTTTTGCAAATCACCTCAATCAATA TCTGCAGGTCGA
	C8	TTTTTTTTTTTTTTTTTTTTTTTTTTTTTTTTTTTTTTTTTTGACGAGCACGTATACTGA AATGGATTATTTAATAAAAG
	C11	TTTTTTTTTTTTTTTTTTTTTTTTTTTTTTTTTTTTTTTTTTATCTAAAGCATCACCTTG CTGATGGCCAAC
	C40	TTTTTTTTTTTTTTTTTTTTTTTTTTTTTTTTTTTTTTTTTTGCCAGTGCGATCCCCGGGT ACCGAGTTTTTCT
Up-T40x5	A1	TTTTTTTTTTTTTTTTTTTTTTTTTTTTTTTTTTTTTTTTTTCGGGGTTTCCTCAAGAGAA GGATTTTGAATTA
	A3	TTTTTTTTTTTTTTTTTTTTTTTTTTTTTTTTTTTTTTTTTTCATAATCCCCTTATTAGC GTTTTTCTTACC
	A8	TTTTTTTTTTTTTTTTTTTTTTTTTTTTTTTTTTTTTTTTTTGACGGGAGAATTAACTCGG AATAAGTTTATTTCCAGCGCC
	A11	TTTTTTTTTTTTTTTTTTTTTTTTTTTTTTTTTTTTTTTTTTCACCGGAAAGCGCGTTTTC ATCGGAAGGGCGA
	A40	TTTTTTTTTTTTTTTTTTTTTTTTTTTTTTTTTTTTTTTTTTAGTATCGCCAACGCTCAA CAGTCGGCTGTC
	B1	TCATATGTGTAATCGTAAAACTAGTCATTTTC
	B3	GGCATCAAATTTGGGGCGCGAGCTAGTTAAAG
	B8	GAATACCACATTCAACTTAAGAGGAAGCCCGATCAAAGCG
	B11	CATCCAATAAATGGTCAATAACCTCGGAAGCA
	B40	ATTCGGTCTGCGGGATCGTCACCCGAAATCCG
	C1	TCGGGAGATATACAGTAACAGTACAAATAATT
	C3	GCAAATCACCTCAATCAATATCTGCAGGTCGA
	C8	TTGACGAGCACGTATACTGAAATGGATTATTTAATAAAAG
	C11	TTATCTAAAGCATCACCTTGCTGATGGCCAAC
	C40	GCCAGTGCGATCCCCGGGTACCGAGTTTTTCT
Loops	Link-A1	TTAATTAATTTTTTACCATATCAAA
	Link-A2	TTAATTTCATCTTAGACTTTACAA
	Link-A3	CTGTCCAGACGTATACCGAACGA
	Link-A4	TCAAGATTAGTGTAGCAATACT
	Link-B1	TGTAGCATTCCTTTTATAAACAGTT

	Link-B2	TTTAATTGTATTTCCACCAGAGCC
	Link-B3	ACTACGAAGGCTTAGCACCATTA
	Link-B4	ATAAGGCTTGCAACAAAGTTAC
	Link-C1	GTGGGAACAAATTTCTATTTTTGAG
	Link-C2	CGGTGCGGGCCTTCCAAAAACATT
	Link-C3	ATGAGTGAGCTTTTAAATATGCA
	Link-C4	ACTATTAAAGAGGATAGCGTCC
	Loop-1	GCGCTTAATGCGCCGCTACAGGGC
GenStock A	A1	CGGGGTTTCCTCAAGAGAAGGATTTTGAATTA
	A2	AGCGTCATGTCTCTGAATTTACCGACTACCTT
	A3	TTCATAATCCCCTTATTAGCGTTTTTCTTACC
	A4	ATGGTTTATGTCACAATCAATAGATATTAAAC
	A6	CCGGAACCCAGAATGGAAAGCGCAACATGGCT
	A7	AAAGACAACATTTTCGGTCATAGCCAAAATCA
	A8	GACGGGAGAATTAACTCGGAATAAGTTTATTTCCAGCGCC
	A11	CACCGGAAAGCGCGTTTTCATCGGAAGGGCGA
	A12	CATTCAACAAACGCAAAGACACCAGAACACCCTGAACAAA
	A14	CTCAGAGCATATTCACAAACAAATTAATAAGT
	A15	GGAGGGAATTTAGCGTCAGACTGTCCGCCTCC
	A16	GTCAGAGGGTAATTGATGGCAACATATAAAAGCGATTGAG
	A18	CCTTGAGTCAGACGATTGGCCTTGCGCCACCC
	A19	TCAGAACCCAGAATCAAGTTTGCCGGTAAATA
	A21	CAGAGCCAGGAGGTTGAGGCAGGTAACAGTGCCCG
	A22	ATTAAAGGCCGTAATCAGTAGCGAGCCACCCT
	A24	GCCGCCAGCATTGACACCACCCTC
	A25	AGAGCCGCACCATCGATAGCAGCATGAATTAT
	A27	AGCCATTTAAACGTCACCAATGAACACCAGAACCA
	A29	CCATTAGCAAGGCCGGGGGAATTA
	A32	CAGAAGGAAACCGAGGTTTTTAAGAAAAGTAAGCAGATAGCCG
	A34	TTTAACCTATCATAGGTCTGAGAGTTCCAGTA
	A36	CAAGTACCTCATTCCAAGAACGGGAAATTCAT
	A40	TTAGTATCGCCAACGCTCAACAGTCGGCTGTC
	A41	TTTCCTTAGCACTCATCGAGAACAATAGCAGCCTTTACAG
	A43	ACTAGAAATATATAACTATATGTACGCTGAGA
	A44	TCAATAATAGGGCTTAATTGAGAATCATAATT
	A47	GATTAAGAAATGCTGATGCAAATCAGAATAAA

	A48	CACCGGAATCGCCATATTTAACAAAATTTACG
	A51	GTTAAATACAATCGCAAGACAAAGCCTTGAAA
	A52	CCCATCCTCGCCAACATGTAATTTAATAAGGC
	A53	TCCCAATCCAAATAAGATTACCGCGCCCAATAAATAATAT
	A54	TCCCTTAGAATAACGCGAGAAAACTTTTACCGACC
	A55	GTGTGATAAGGCAGAGGCATTTTCAGTCCTGA
	A56	ACAAGAAAGCAAGCAAATCAGATAACAGCCATATTATTTA
	A57	GTTTGAAATTCAAATATATTTTAG
	A58	AATAGATAGAGCCAGTAATAAGAGATTTAATG
	A60	TTCTGACCTAAAATATAAAGTACCGACTGCAGAAC
	A62	TCAGCTAAAAAAGGTAAAGTAATT
	A65	TGCTATTTTGCACCCAGCTACAATTTTGTTTTGAAGCCTTAAA
	B01	TCATATGTGTAATCGTAAAACTAGTCATTTTC
	B02	GTGAGAAAATGTGTAGGTAAAGATACAACTTT
	B03	GGCATCAAATTTGGGGCGCGAGCTAGTTAAAG
	B04	TTCGAGCTAAGACTTCAAATATCGGGAACGAG
	B06	ATAGTAGTATGCAATGCCTGAGTAGGCCGGAG
	B07	AACCAGACGTTTAGCTATATTTTCTTCTACTA
	B08	GAATACCACATTCAACTTAAGAGGAAGCCCGATCAAAGCG
	B11	CATCCAATAAATGGTCAATAACCTCGGAAGCA
	B12	AACTCCAAGATTGCATCAAAAAGATAATGCAGATACATAA
	B14	CAGGCAAGATAAAAATTTTTAGAATATTCAAC
	B15	GATTAGAGATTAGATACATTTCGCAAATCATA
	B16	CGCCAAAAGGAATTACAGTCAGAAGCAAAGCGCAGGTCAG
	B18	TTAATGCCTTATTTCAACGCAAGGGCAAAGAA
	B19	TTAGCAAATAGATTTAGTTTGACCAGTACCTT
	B21	ATAAAGCCTTTGCGGGAGAAGCCTGGAGAGGGTAG
	B22	TAAGAGGTCAATTCTGCGAACGAGATTAAGCA
	B24	ATGACCCTGTAATACTTCAGAGCA
	B25	TAAAGCTATATAACAGTTGATTCCCATTTTTG
	B27	TAATTGCTTGGAAGTTTCATTCCAAATCGGTTGTA
	B29	ACTAAAGTACGGTGTCGAATATAA
	B32	AATACTGCGGAATCGTAGGGGGTAATAGTAAAATGTTTAGACT
	B34	CAACAGTTTATGGGATTTTGCTAATCAAAAGG
	B36	GCGCAGACTCCATGTTACTTAGCCCGTTTTAA
	B40	ATTCGGTCTGCGGGATCGTCACCCGAAATCCG
	B41	CGACCTGCGGTCAATCATAAGGGAACGGAACAACATTATT
	B43	CACGCATAAGAAAGGAACAACTAAGTCTTTCC
	B44	ATTGTGTCTCAGCAGCGAAAGACACCATCGCC
	B47	GTTTTGTCAGGAATTGCGAATAATCCGACAAT
	B48	GACAACAAGCATCGGAACGAGGGTGAGATTTG

	B51	TAGTTGCGAATTTTTTCACGTTGATCATAGTT
	B52	GTACAACGAGCAACGGCTACAGAGGATACCGA
	B53	ACCAGTCAGGACGTTGGAACGGTGTACAGACCGAAACAAA
	B54	ACAGACAGCCCAAATCTCCAAAAAAAAATTTCTTA
	B55	AACAGCTTGCTTTGAGGACTAAAGCGATTATA
	B56	CCAAGCGCAGGCGCATAGGCTGGCAGAACTGGCTCATTAT
	B57	CGAGGTGAGGCTCCAAAAGGAGCC
	B58	ACCCCCAGACTTTTTCATGAGGAACTTGCTTT
	B60	CGGTTTATCAGGTTTCCATTAAACGGGAATACACT
	B62	GGCAAAAGTAAAATACGTAATGCC
	B65	CCTGACGAGAAACACCAGAACGAGTAGGCTGCTCATTCAGTGA
	C01	TCGGGAGATATACAGTAACAGTACAAATAATT
	C02	CCTGATTAAAGGAGCGGAATTATCTCGGCCTC
	C03	GCAAATCACCTCAATCAATATCTGCAGGTCGA
	C04	CGACCAGTACATTGGCAGATTCACCTGATTGC
	C06	AAGGAATTACAAAGAAACCACCAGTCAGATGA
	C07	GGACATTCACCTCAAATATCAAACACAGTTGA
	C08	TTGACGAGCACGTATACTGAAATGGATTATTTAATAAAAG
	C11	TTATCTAAAGCATCACCTTGCTGATGGCCAAC
	C12	AGAGATAGTTTGACGCTCAATCGTACGTGCTTTCCTCGTT
	C14	TAGGAGCATAAAAGTTTGAGTAACATTGTTTG
	C15	TGACCTGACAAATGAAAAATCTAAAATATCTT
	C16	AGAATCAGAGCGGGAGATGGAAATACCTACATAACCCTTC
	C18	AATGGAAGCGAACGTTATTAATTTCTAACAAC
	C19	TAATAGATCGCTGAGAGCCAGCAGAAGCGTAA
	C21	TCAATAGATATTAAATCCTTTGCCGGTTAGAACCT
	C22	CAATATTTGCCTGCAACAGTGCCATAGAGCCG
	C24	ACAATTCGACAACTCGTAATACAT
	C25	TTGAGGATGGTCAGTATTAACACCTTGAATGG
	C27	CGCGAACTAAAACAGAGGTGAGGCTTAGAAGTATT
	C29	ACCACCAGCAGAAGATGATAGCCC
	C32	TCTTTGATTAGTAATAGTCTGTCCATCACGCAAATTAACCGTT
	C34	AGGAAGATGGGGACGACGACAGTAATCATATT
	C36	CCTTCACCGTGAGACGGGCAACAGCAGTCACA
	C40	GCCAGTGCGATCCCCGGGTACCGAGTTTTTCT
	C41	TTTCACCAGCCTGGCCCTGAGAGAAAGCCGGCGAACGTGG
	C43	ACGTTGTATTCCGGCACCGCTTCTGGCGCATC
	C44	CCAGGGTGGCTCGAATTCGTAATCCAGTCACG
	C47	TGTAGATGGGTGCCGGAAACCAGGAACGCCAG
	C48	GGTTTTCCATGGTCATAGCTGTTTGAGAGGCG
	C51	AGTTGGGTCAAAGCGCCATTCGCCCCGTAATG

	C52	CGCGCGGGCCTGTGTGAAATTGTTGGCGATTA
	C53	CTAAATCGGAACCCTAAGCAGGCGAAAATCCTTCGGCCAA
	C54	CGGCGGATTGAATTCAGGCTGCGCAACGGGGGATG
	C55	TGCTGCAAATCCGCTCACAATTCCCAGCTGCA
	C56	TTAATGAAGTTTGATGGTGGTTCCGAGGTGCCGTAAAGCA
	C57	TGGCGAAATGTTGGGAAGGGCGAT
	C58	TGTCGTGCACACAACATACGAGCCACGCCAGC
	C61	TTCCAGTCCTTATAAATCAAAAGAGAACCATCACCCAAAT
	C62	GCGCTCACAAGCCTGGGGTGCCTA
	C65	ACGTGGACTCCAACGTCAAAGGGCGAATTTGGAACAAGAGTCC
GenStock B	Name	Sequence
	A2	AGCGTCATGTCTCTGAATTTACCGACTACCTT
	A4	ATGGTTTATGTCACAATCAATAGATATTAAAC
	A5	TTTGATGATTAAGAGGCTGAGACTTGCTCAGTACCAGGCG
	A6	CCGGAACCCAGAATGGAAAGCGCAACATGGCT
	A7	AAAGACAACATTTTCGGTCATAGCCAAAATCA
	A9	GATAAGTGCCGTCGAGCTGAAACATGAAAGTATACAGGAG
	A10	TGTACTGGAAATCCTCATTAAAGCAGAGCCAC
	A12	CATTCAACAAACGCAAAGACACCAGAACACCCTGAACAAA
	A13	TTTAACGGTTCGGAACCTATTATTAGGGTTGATATAAGTA
	A14	CTCAGAGCATATTCACAAACAAATTAATAAGT
	A15	GGAGGGAATTTAGCGTCAGACTGTCCGCCTCC
	A16	GTCAGAGGGTAATTGATGGCAACATATAAAAGCGATTGAG
	A17	TAGCCCGGAATAGGTGAATGCCCCCTGCCTATGGTCAGTG
	A18	CCTTGAGTCAGACGATTGGCCTTGCGCCACCC
	A19	TCAGAACCCAGAATCAAGTTTGCCGGTAAATA
	A20	TTGACGGAAATACATACATAAAGGGCGCTAATATCAGAGA
	A21	CAGAGCCAGGAGGTTGAGGCAGGTAACAGTGCCCG
	A22	ATTAAAGGCCGTAATCAGTAGCGAGCCACCCT
	A23	GATAACCCACAAGAATGTTAGCAAACGTAGAAAATTATTC
	A24	GCCGCCAGCATTGACACCACCCTC
	A25	AGAGCCGCACCATCGATAGCAGCATGAATTAT
	A26	CACCGTCACCTTATTACGCAGTATTGAGTTAAGCCCAATA
	A27	AGCCATTTAAACGTCACCAATGAACACCAGAACCA
	A28	ATAAGAGCAAGAAACATGGCATGATTAAGACTCCGACTTG
	A29	CCATTAGCAAGGCCGGGGGAATTA
	A30	GAGCCAGCGAATACCCAAAAGAACATGAAATAGCAATAGC
	A31	TATCTTACCGAAGCCCAAACGCAATAATAACGAAAATCACCAG
	A32	CAGAAGGAAACCGAGGTTTTTAAGAAAAGTAAGCAGATAGCCG
	A33	CCTTTTTTCATTTAACAATTTCATAGGATTAG

	A34	TTTAACCTATCATAGGTCTGAGAGTTCCAGTA
	A35	AGTATAAAATATGCGTTATACAAAGCCATCTT
	A36	CAAGTACCTCATTCCAAGAACGGGAAATTCAT
	A37	AGAGAATAACATAAAAACAGGGAAGCGCATTA
	A38	AAAACAAAATTAATTAAATGGAAACAGTACATTAGTGAAT
	A39	TTATCAAACCGGCTTAGGTTGGGTAAGCCTGT
	A41	TTTCCTTAGCACTCATCGAGAACAATAGCAGCCTTTACAG
	A42	AGAGTCAAAAATCAATATATGTGATGAAACAAACATCAAG
	A43	ACTAGAAATATATAACTATATGTACGCTGAGA
	A44	TCAATAATAGGGCTTAATTGAGAATCATAATT
	A45	AACGTCAAAAATGAAAAGCAAGCCGTTTTTATGAAACCAA
	A46	GAGCAAAAGAAGATGAGTGAATAACCTTGCTTATAGCTTA
	A47	GATTAAGAAATGCTGATGCAAATCAGAATAAA
	A48	CACCGGAATCGCCATATTTAACAAAATTTACG
	A49	AGCATGTATTTCATCGTAGGAATCAAACGATTTTTTGTTT
	A50	ACATAGCGCTGTAAATCGTCGCTATTCATTTCAATTACCT
	A51	GTTAAATACAATCGCAAGACAAAGCCTTGAAA
	A52	CCCATCCTCGCCAACATGTAATTTAATAAGGC
	A53	TCCCAATCCAAATAAGATTACCGCGCCCAATAAATAATAT
	A54	TCCCTTAGAATAACGCGAGAAAACTTTTACCGACC
	A55	GTGTGATAAGGCAGAGGCATTTTCAGTCCTGA
	A56	ACAAGAAAGCAAGCAAATCAGATAACAGCCATATTATTTA
	A57	GTTTGAAATTCAAATATATTTTAG
	A58	AATAGATAGAGCCAGTAATAAGAGATTTAATG
	A59	GCCAGTTACAAAATAATAGAAGGCTTATCCGGTTATCAAC
	A60	TTCTGACCTAAAATATAAAGTACCGACTGCAGAAC
	A61	GCGCCTGTTATTCTAAGAACGCGATTCCAGAGCCTAATTT
	A62	TCAGCTAAAAAAGGTAAAGTAATT
	A63	ACGCTAACGAGCGTCTGGCGTTTTAGCGAACCCAACATGT
	A64	ACGACAATAAATCCCGACTTGCGGGAGATCCTGAATCTTACCA
	A65	TGCTATTTTGCACCCAGCTACAATTTTGTTTTGAAGCCTTAAA
	B02	GTGAGAAAATGTGTAGGTAAAGATACAACTTT
	B04	TTCGAGCTAAGACTTCAAATATCGGGAACGAG
	B5	ACAGTCAAAGAGAATCGATGAACGACCCCGGTTGATAATC
	B06	ATAGTAGTATGCAATGCCTGAGTAGGCCGGAG
	B07	AACCAGACGTTTAGCTATATTTTCTTCTACTA
	B9	AGAAAAGCCCCAAAAAGAGTCTGGAGCAAACAATCACCAT
	B10	CAATATGACCCTCATATATTTTAAAGCATTAA
	B12	AACTCCAAGATTGCATCAAAAAGATAATGCAGATACATAA
	B13	CGTTCTAGTCAGGTCATTGCCTGACAGGAAGATTGTATAA
	B14	CAGGCAAGATAAAAATTTTTAGAATATTCAAC

	B15	GATTAGAGATTAGATACATTTCGCAAATCATA
	B16	CGCCAAAAGGAATTACAGTCAGAAGCAAAGCGCAGGTCAG
	B17	GCAAATATTTAAATTGAGATCTACAAAGGCTACTGATAAA
	B18	TTAATGCCTTATTTCAACGCAAGGGCAAAGAA
	B19	TTAGCAAATAGATTTAGTTTGACCAGTACCTT
	B20	TAATTGCTTTACCCTGACTATTATGAGGCATAGTAAGAGC
	B21	ATAAAGCCTTTGCGGGAGAAGCCTGGAGAGGGTAG
	B22	TAAGAGGTCAATTCTGCGAACGAGATTAAGCA
	B23	AACACTATCATAACCCATCAAAAATCAGGTCTCCTTTTGA
	B24	ATGACCCTGTAATACTTCAGAGCA
	B25	TAAAGCTATATAACAGTTGATTCCCATTTTTG
	B26	CGGATGGCACGAGAATGACCATAATCGTTTACCAGACGAC
	B27	TAATTGCTTGGAAGTTTCATTCCAAATCGGTTGTA
	B28	GATAAAAACCAAAATATTAAACAGTTCAGAAATTAGAGCT
	B29	ACTAAAGTACGGTGTCGAATATAA
	B30	TGCTGTAGATCCCCCTCAAATGCTGCGAGAGGCTTTTGCA
	B31	AAAGAAGTTTTGCCAGCATAAATATTCATTGACTCAACATGTT
	B32	AATACTGCGGAATCGTAGGGGGTAATAGTAAAATGTTTAGACT
	B33	AGGGATAGCTCAGAGCCACCACCCCATGTCAA
	B34	CAACAGTTTATGGGATTTTGCTAATCAAAAGG
	B35	GCCGCTTTGCTGAGGCTTGCAGGGGAAAAGGT
	B36	GCGCAGACTCCATGTTACTTAGCCCGTTTTAA
	B37	ACAGGTAGAAAGATTCATCAGTTGAGATTTAG
	B38	CCTCAGAACCGCCACCCAAGCCCAATAGGAACGTAAATGA
	B39	ATTTTCTGTCAGCGGAGTGAGAATACCGATAT
	B41	CGACCTGCGGTCAATCATAAGGGAACGGAACAACATTATT
	B42	AGACGTTACCATGTACCGTAACACCCCTCAGAACCGCCAC
	B43	CACGCATAAGAAAGGAACAACTAAGTCTTTCC
	B44	ATTGTGTCTCAGCAGCGAAAGACACCATCGCC
	B45	TTAATAAAACGAACTAACCGAACTGACCAACTCCTGATAA
	B46	AGGTTTAGTACCGCCATGAGTTTCGTCACCAGGATCTAAA
	B47	GTTTTGTCAGGAATTGCGAATAATCCGACAAT
	B48	GACAACAAGCATCGGAACGAGGGTGAGATTTG
	B49	TATCATCGTTGAAAGAGGACAGATGGAAGAAAAATCTACG
	B50	AGCGTAACTACAAACTACAACGCCTATCACCGTACTCAGG
	B51	TAGTTGCGAATTTTTTCACGTTGATCATAGTT
	B52	GTACAACGAGCAACGGCTACAGAGGATACCGA
	B53	ACCAGTCAGGACGTTGGAACGGTGTACAGACCGAAACAAA
	B54	ACAGACAGCCCAAATCTCCAAAAAAAAATTTCTTA
	B55	AACAGCTTGCTTTGAGGACTAAAGCGATTATA
	B56	CCAAGCGCAGGCGCATAGGCTGGCAGAACTGGCTCATTAT

	B57	CGAGGTGAGGCTCCAAAAGGAGCC
	B58	ACCCCCAGACTTTTTCATGAGGAACTTGCTTT
	B59	ACCTTATGCGATTTTATGACCTTCATCAAGAGCATCTTTG
	B60	CGGTTTATCAGGTTTCCATTAAACGGGAATACACT
	B61	AAAACACTTAATCTTGACAAGAACTTAATCATTGTGAATT
	B62	GGCAAAAGTAAAATACGTAATGCC
	B63	TGGTTTAATTTCAACTCGGATATTCATTACCCACGAAAGA
	B64	ACCAACCTAAAAAATCAACGTAACAAATAAATTGGGCTTGAGA
	B65	CCTGACGAGAAACACCAGAACGAGTAGGCTGCTCATTCAGTGA
	C02	CCTGATTAAAGGAGCGGAATTATCTCGGCCTC
	C04	CGACCAGTACATTGGCAGATTCACCTGATTGC
	C5	TGGCAATTTTTAACGTCAGATGAAAACAATAACGGATTCG
	C06	AAGGAATTACAAAGAAACCACCAGTCAGATGA
	C07	GGACATTCACCTCAAATATCAAACACAGTTGA
	C9	CCTGATTGCTTTGAATTGCGTAGATTTTCAGGCATCAATA
	C10	TAATCCTGATTATCATTTTGCGGAGAGGAAGG
	C12	AGAGATAGTTTGACGCTCAATCGTACGTGCTTTCCTCGTT
	C13	GATTATACACAGAAATAAAGAAATACCAAGTTACAAAATC
	C14	TAGGAGCATAAAAGTTTGAGTAACATTGTTTG
	C15	TGACCTGACAAATGAAAAATCTAAAATATCTT
	C16	AGAATCAGAGCGGGAGATGGAAATACCTACATAACCCTTC
	C17	GCGCAGAGGCGAATTAATTATTTGCACGTAAATTCTGAAT
	C18	AATGGAAGCGAACGTTATTAATTTCTAACAAC
	C19	TAATAGATCGCTGAGAGCCAGCAGAAGCGTAA
	C20	GAATACGTAACAGGAAAAACGCTCCTAAACAGGAGGCCGA
	C21	TCAATAGATATTAAATCCTTTGCCGGTTAGAACCT
	C22	CAATATTTGCCTGCAACAGTGCCATAGAGCCG
	C23	TTAAAGGGATTTTAGATACCGCCAGCCATTGCGGCACAGA
	C24	ACAATTCGACAACTCGTAATACAT
	C25	TTGAGGATGGTCAGTATTAACACCTTGAATGG
	C26	CTATTAGTATATCCAGAACAATATCAGGAACGGTACGCCA
	C27	CGCGAACTAAAACAGAGGTGAGGCTTAGAAGTATT
	C28	GAATCCTGAGAAGTGTATCGGCCTTGCTGGTACTTTAATG
	C29	ACCACCAGCAGAAGATGATAGCCC
	C30	TAAAACATTAGAAGAACTCAAACTTTTTATAATCAGTGAG
	C31	GCCACCGAGTAAAAGAACATCACTTGCCTGAGCGCCATTAAAA
	C32	TCTTTGATTAGTAATAGTCTGTCCATCACGCAAATTAACCGTT
	C33	CGCGTCTGATAGGAACGCCATCAACTTTTACA
	C34	AGGAAGATGGGGACGACGACAGTAATCATATT
	C35	CTCTAGAGCAAGCTTGCATGCCTGGTCAGTTG
	C36	CCTTCACCGTGAGACGGGCAACAGCAGTCACA

	C37	CGAGAAAGGAAGGGAAGCGTACTATGGTTGCT
	C38	GCTCATTTTTTAACCAGCCTTCCTGTAGCCAGGCATCTGC
	C39	CAGTTTGACGCACTCCAGCCAGCTAAACGACG
	C41	TTTCACCAGCCTGGCCCTGAGAGAAAGCCGGCGAACGTGG
	C42	GTAACCGTCTTTCATCAACATTAAAATTTTTGTTAAATCA
	C43	ACGTTGTATTCCGGCACCGCTTCTGGCGCATC
	C44	CCAGGGTGGCTCGAATTCGTAATCCAGTCACG
	C45	TAGAGCTTGACGGGGAGTTGCAGCAAGCGGTCATTGGGCG
	C46	GTTAAAATTCGCATTAATGTGAGCGAGTAACACACGTTGG
	C47	TGTAGATGGGTGCCGGAAACCAGGAACGCCAG
	C48	GGTTTTCCATGGTCATAGCTGTTTGAGAGGCG
	C49	GTTTGCGTCACGCTGGTTTGCCCCAAGGGAGCCCCCGATT
	C50	GGATAGGTACCCGTCGGATTCTCCTAAACGTTAATATTTT
	C51	AGTTGGGTCAAAGCGCCATTCGCCCCGTAATG
	C52	CGCGCGGGCCTGTGTGAAATTGTTGGCGATTA
	C53	CTAAATCGGAACCCTAAGCAGGCGAAAATCCTTCGGCCAA
	C54	CGGCGGATTGAATTCAGGCTGCGCAACGGGGGATG
	C55	TGCTGCAAATCCGCTCACAATTCCCAGCTGCA
	C56	TTAATGAAGTTTGATGGTGGTTCCGAGGTGCCGTAAAGCA
	C57	TGGCGAAATGTTGGGAAGGGCGAT
	C58	TGTCGTGCACACAACATACGAGCCACGCCAGC
	C59	CAAGTTTTTTGGGGTCGAAATCGGCAAAATCCGGGAAACC
	C60	TCTTCGCTATTGGAAGCATAAAGTGTATGCCCGCT
	C61	TTCCAGTCCTTATAAATCAAAAGAGAACCATCACCCAAAT
	C62	GCGCTCACAAGCCTGGGGTGCCTA
	C63	CGATGGCCCACTACGTATAGCCCGAGATAGGGATTGCGTT
	C64	AACTCACATTATTGAGTGTTGTTCCAGAAACCGTCTATCAGGG
	C65	ACGTGGACTCCAACGTCAAAGGGCGAATTTGGAACAAGAGTCC

Up-TGAx15	A10	TGTACTGGAAATCCTCATTAAAGCAGAGCCACTTTGATGATGATGATGATGATGA
	A33	CCTTTTTTCATTTAACAATTTCATAGGATTAGTTTGATGATGATGATGATGATGA
	A35	AGTATAAAATATGCGTTATACAAAGCCATCTTTTTGATGATGATGATGATGATGA
	A37	AGAGAATAACATAAAAACAGGGAAGCGCATTTTTGATGATGATGATGATGATGAA
	A39	TTATCAAACCGGCTTAGGTTGGGTAAGCCTGTTTTGATGATGATGATGATGATGA
	B10	CAATATGACCCTCATATATTTTAAAGCATTTTTGATGATGATGATGATGATGAAA
	B33	AGGGATAGCTCAGAGCCACCACCCCATGTCTTTGATGATGATGATGATGATGAAA
	B35	GCCGCTTTGCTGAGGCTTGCAGGGGAAAAGGTTTTGATGATGATGATGATGATGA

	B37	ACAGGTAGAAAGATTCATCAGTTGAGATTTAGTTTGATGATGATGATGATGATGA
	B39	ATTTTCTGTCAGCGGAGTGAGAATACCGATATTTTGATGATGATGATGATGATGA
	C10	TAATCCTGATTATCATTTTGCGGAGAGGAAGGTTTGATGATGATGATGATGATGA
	C33	CGCGTCTGATAGGAACGCCATCAACTTTTACTTTGATGATGATGATGATGATGAA
	C35	CTCTAGAGCAAGCTTGCATGCCTGGTCAGTTGTTTGATGATGATGATGATGATGA
	C37	CGAGAAAGGAAGGGAAGCGTACTATGGTTGCTTTTGATGATGATGATGATGATGA
	C39	CAGTTTGACGCACTCCAGCCAGCTAAACGACGTTTGATGATGATGATGATGATGA

Side -A40	A61	GCGCCTGTTATTCTAAGAACGCGATTCCAGAGCCTAATTTGCCAGTTACAATA AAAAAAAAAAAAAAAAAAAAAAAAAAAAAAAAAAAAAA
	A49	AGCATGTATTTCATCGTAGGAATCAAACGATTTTTTGTTTAACGTCAAAAATAA AAAAAAAAAAAAAAAAAAAAAAAAAAAAAAAAAAAAAA
	A20	TTGACGGAAATACATACATAAAGGGCGCTAATATCAGAGAGATAACCCACAT AAAAAAAAAAAAAAAAAAAAAAAAAAAAAAAAAAAAAA
	A30	GAGCCAGCGAATACCCAAAAGAACATGAAATAGCAATAGCTATCTTACCGAT AAAAAAAAAAAAAAAAAAAAAAAAAAAAAAAAAAAAAA
	B61	AAAACACTTAATCTTGACAAGAACTTAATCATTGTGAATTACCTTATGCGATAA AAAAAAAAAAAAAAAAAAAAAAAAAAAAAAAAAAAAAA
	B49	TATCATCGTTGAAAGAGGACAGATGGAAGAAAAATCTACGTTAATAAAACGTA AAAAAAAAAAAAAAAAAAAAAAAAAAAAAAAAAAAAAA
	B20	TAATTGCTTTACCCTGACTATTATGAGGCATAGTAAGAGCAACACTATCATTA AAAAAAAAAAAAAAAAAAAAAAAAAAAAAAAAAAAAAA
	B30	TGCTGTAGATCCCCCTCAAATGCTGCGAGAGGCTTTTGCAAAAGAAGTTTTT AAAAAAAAAAAAAAAAAAAAAAAAAAAAAAAAAAAAAA
	C61	TTCCAGTCCTTATAAATCAAAAGAGAACCATCACCCAAATCAAGTTTTTTGTAA AAAAAAAAAAAAAAAAAAAAAAAAAAAAAAAAAAAAAA
	C49	GTTTGCGTCACGCTGGTTTGCCCCAAGGGAGCCCCCGATTTAGAGCTTGAC TAAAAAAAAAAAAAAAAAAAAAAAAAAAAAAAAAAAAAA
	C20	GAATACGTAACAGGAAAAACGCTCCTAAACAGGAGGCCGATTAAAGGGATTT AAAAAAAAAAAAAAAAAAAAAAAAAAAAAAAAAAAAAA
	C30	TAAAACATTAGAAGAACTCAAACTTTTTATAATCAGTGAGGCCACCGAGTATA AAAAAAAAAAAAAAAAAAAAAAAAAAAAAAAAAAAAAA
	A59	AATAATAGAAGGCTTATCCGGTTATCAAC
	A45	TGAAAAGCAAGCCGTTTTTATGAAACCAA
	A23	AGAATGTTAGCAAACGTAGAAAATTATTC
	A31	AGCCCAAACGCAATAATAACGAAAATCACCAG
	B59	TTTTATGACCTTCATCAAGAGCATCTTTG
	B45	AACTAACCGAACTGACCAACTCCTGATAA
	B23	AACCCATCAAAAATCAGGTCTCCTTTTGA
	B31	GCCAGCATAAATATTCATTGACTCAACATGTT
	C59	GGGTCGAAATCGGCAAAATCCGGGAAACC
	C45	GGGGAGTTGCAGCAAGCGGTCATTGGGCG
	C23	TTAGATACCGCCAGCCATTGCGGCACAGA
	C31	AAAGAACATCACTTGCCTGAGCGCCATTAAAA

Additional strands

“Anti-strand” sequence:
GGAAGTCTGATGATGATGATGATGATGAAAAA

“MB-strand” sequence:
T*TTTTCATCATCATCATCATCATCAGACTTCC
T*=methylene blue dT

Fig. S19. Illustration: MB-strand design, toehold position and effect of anti-strand addition.

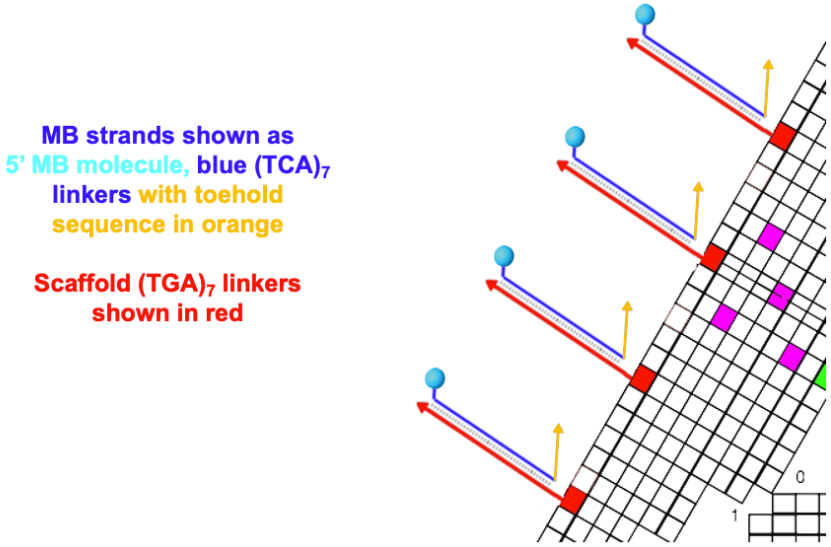

The single-stranded anti-toehold region (orange) on the anti strand binds the single-stranded toehold sequence on the MB strand(orange). Once bound, branch migation enables the anti-strand to displace the MB strand as shown below. 1/1* and 2/2* refer to sequence/watson-crick-complement sequence.

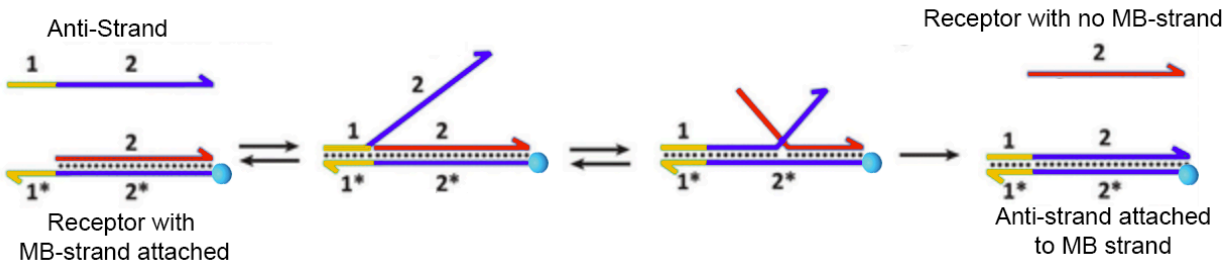

References

1. A. M. Hung, C. M. Micheel, L. D. Bozano, L. W. Osterbur, G. M. Wallraff and J. N. Cha, *Nature nanotechnology*, 2010, **5**, 121.
2. D. Qu, B.-C. Kim, C.-W. J. Lee, M. Ito, H. Noguchi and K. Uosaki, *The Journal of Physical Chemistry C*, 2010, **114**, 497-505.
3. M. A. D. Millone, H. Hamoudi, L. Rodríguez, A. Rubert, G. A. Benítez, M. E. Vela, R. C. Salvarezza, J. E. Gayone, E. A. Sánchez, O. Grizzi, C. Dablemont and V. A. Esaulov, *Langmuir*, 2009, **25**, 12945-12953.
4. P. Kohli, K. K. Taylor, J. J. Harris and G. J. Blanchard, *Journal of the American Chemical Society*, 1998, **120**, 11962-11968.
5. J. F. Smalley, S. W. Feldberg, C. E. D. Chidsey, M. R. Linford, M. D. Newton and Y.-P. Liu, *The Journal of Physical Chemistry*, 1995, **99**, 13141-13149.
6. K. F. Wagenbauer, F. A. S. Engelhardt, E. Stahl, V. K. Hechtl, P. Stömmer, F. Seebacher, L. Meregalli, P. Ketterer, T. Gerling and H. Dietz, *ChemBioChem*, 2017, **18**, 1873-1885.
7. R. J. White, N. Phares, A. A. Lubin, Y. Xiao and K. W. Plaxco, *Langmuir : the ACS journal of surfaces and colloids*, 2008, **24**, 10513-10518.
8. S. Trasatti and O. A. Petrii, *Pure and Applied Chemistry*, 1991, **63**, 711-734.
9. J. S. Schreck, F. Romano, M. H. Zimmer, A. A. Louis and J. P. Doye, *ACS nano*, 2016, **10**, 4236-4247.
10. B. E. Snodin, F. Romano, L. Rovigatti, T. E. Ouldridge, A. A. Louis and J. P. Doye, *ACS nano*, 2016, **10**, 1724-1737.
11. Z. Shi, C. E. Castro and G. Arya, *ACS nano*, 2017, **11**, 4617-4630.
12. R. Sharma, J. S. Schreck, F. Romano, A. A. Louis and J. P. Doye, *ACS nano*, 2017, **11**, 12426-12435.
13. C.-M. Huang, A. Kucinic, J. V. Le, C. E. Castro and H.-J. Su, *Nanoscale*, 2019, **11**, 1647-1660.